Velasquez MT, Kimmel PL, Michaelis OE IV. 1990. Animal models of spontaneous diabetic kidney disease. FASEB J 4:2850–2859.
Wang T, Fontenot RD, Soni MG, Bucci TJ, Mehendale HM. 2000. Enhanced hepatotoxicity and toxic outcome of thioacetamide in streptozotocin-induced diabetic rats. Toxicol Appl Pharmacol 166:92–100.
Williamson JR, Chang K, Tilton RG, Prater C, Jeffrey JR, Weigel C, Sherman WR, Eades DM, Kilo C. 1987. Increased vascular permeability in spontaneously diabetic BB/W rats and in rats with mild versus severe streptozocin-induced diabetes. Prevention by aldose reductase inhibitors and castration. Diabetes 36:813–821.
Yokozawa T, Nakagawa T, Wakaki K, Koizumi F. 2001. Animal model of diabetic nephropathy. Exp Toxicol Pathol 53:359–363.
Zatz R, Meyer TW, Rennke HG, Brenner BM. 1985. Predominance of hemodynamic rather than metabolic factors in the pathogenesis of diabetic glomerulopathy. Proc Natl Acad Sci USA 82:5963–5967.

A comparative study of the diagnostic accuracy of ELISA systems for the detection of anti-neutrophil cytoplasm antibodies available in Japan and Europe

T. Ito-Ihara[1,2,3], E. Muso[1], S. Kobayashi[4], K. Uno[2], N. Tamura[5], Y. Yamanishi[6], A. Fukatsu[7], R.A. Watts[8], D.G.I. Scott[9], D.R.W. Jayne[10], K. Suzuki[11], H. Hashimoto[5]

[1]Department of Nephrology and Dialysis, Kitano Hospital, Tazuke Kofukai Medical Research Institute, Osaka, Japan; [2]Louis Pasteur Centre for Medical Research, Kyoto, Japan; [3]Musculoskeletal Research Group, School of Clinical Medical Sciences, Newcastle University, Newcastle upon Tyne, UK; [4]Department of Rheumatology, Juntendo Koshigaya Hospital, Saitama, Japan; [5]Department of Internal Medicine and Rheumatology, Juntendo University, School of Medicine, Tokyo, Japan; [6]Department of Rheumatology, Hiroshima City Hospital, Hiroshima, Japan; [7]Department of Nephrology, Kyoto University Graduate School of Medicine, Kyoto, Japan; [8]Department of Rheumatology, Ipswich Hospital, Suffolk, UK; [9]Department of Rheumatology, Norfolk and Norwich University Hospital, Norfolk, UK; [10]Lupus and Vasculitis Clinic, Addenbrookes' Hospital, Cambridge, UK; [11]National Institute of Infectious Diseases (NIID-NIH), Tokyo, Japan and Chiba University Graduate School of Medicine, Inflammation Program, Department of Immunology, Chiba, Japan.

Abstract

Objectives

Primary systemic vasculitis associated with anti-neutrophil cytoplasm antibodies (ANCA) differs in its frequency and clinical expression between Japan and Europe. We sought to ascertain whether such differences arise from the performance of enzyme-linked immunosorbent assays (ELISAs) for ANCA.

Methods

Plasma samples from 64 consecutive Japanese patients with a clinical and histological diagnosis of primary systemic vasculitis including microscopic polyangiitis (MPA; n=52), Churg-Strauss syndrome (CSS; n=1), and Wegener's granulomatosis (WG; n=11), or those from disease controls with non-vasculitic glomerulonephritis (n=54) and healthy controls (n=55) were tested for the presence of myeloperoxidase (MPO) by ELISAs available in Japan (Nipro and MBL) and compared with those in Europe (Wieslab). The sensitivity and specificity were calculated for each ELISA, and its diagnostic performance was assessed by receiver operating characteristic curve analysis.

Results

The sensitivity and specificity of either MPO-ANCA assays for a diagnosis of MPA were 90.4% and 98.2% (Nipro), 88.2% and 96.3% (MBL), and 86.5% and 99.1% (Wieslab). The overall diagnostic performance, assessed as the area under curve of the MPO-ANCA ELISAs for MPA were 0.946±0.022 (Nipro), 0.970±0.017 (MBL), and 0.971±0.017 (Wieslab), while that of PR3-ANCA ELISAs for WG were 0.986±0.025 (Nipro), 0.993±0.017 (MBL), and 0.916±0.059 (Wieslab).

Conclusions

The MPO-ANCA ELISAs commercially available in Japan exhibited high sensitivity and specificity for the diagnosis of ANCA-associated vasculitides and provided similar diagnostic value to those in Europe. These results facilitate further international comparison of ANCA-associated vasculitides between Japanese and European populations.

Key words

MPO-ANCA, PR3-ANCA, Capture ELISA, streptavidin-coated ELISA, ANCA-associated vasculitides (AAV), systemic vasculitis.

Clinical and Experimental Rheumatology 2008; **26**: 1027-1033.

Toshiko Ito-Ihara MD, PhD
Eri Muso MD, PhD
Shigeto Kobayashi MD, PhD
Kazuko Uno PhD
Naoto Tamura MD, PhD
Yuji Yamanishi MD, PhD
Atsushi Fukatsu MD, PhD
Richard A. Watts DM
David G.I. Scott MD, FRCP
David R.W. Jayne MD, FRCP
Kazuo Suzuki PhD
Hiroshi Hashimoto MD, PhD

This study was supported by grant no. SH44410, the Japan Health Sciences Foundation with a grant for "Research on Health Sciences focusing on Drug Innovation, International Collaborative Research", the Ministry of Health, Labour and Welfare in Japan from 2004 to 2006; a grant for "Research on Regulatory Science of Pharmaceuticals and Medical Devices", the Ministry of Health, Labour and Welfare in Japan; the "Dispatch program Abroad for Japanese Researchers 2006" from the Society of Japanese Pharmacopoeia; a research grant from Japan Society for Promotion Science and Ministry of Education, Culture, Sports, Science and Technology, Grant in Aid for Young Scientists (B) no. 18790584 (to T.I.); the British Council Japan Association Fellowship 2007 (to T.I.); and the Daiwa Foundation Small Grant from The Daiwa Anglo-Japanese Foundation (to T.I., D.J., E.M.).

Please address reprint requests and correspondence to:
Professor Eri Muso,
The Tazuke Kofukai Medical Research Institute, Kitano Hospital,
2-4-20 Ogimachi, Kitaku, Osaka, 530-8480, Japan.
E-mail: muso@kitano-hp.or.jp

Received on October 15, 2007; accepted in revised form on May 30, 2008.

Competing interests: none declared.

Introduction

Anti-neutrophil cytotoplasm antibodies (ANCA) are found in a high percentage of patients with Wegener's granulomatosis (WG), microscopic polyangiitis (MPA) and Churg-Strauss syndrome (CSS) and are used as diagnostic markers for these diseases, which are also termed the ANCA-associated vasculitides (AAV). On the indirect immunofluorescence (IIF) test, ANCA usually exhibits either a granular cytoplasmic pattern (C-ANCA) or a peri-nuclear pattern (P-ANCA). C-ANCA positivity is characteristically observed in patients with WG mostly directed against proteinase 3 (PR3-ANCA), while the P-ANCA that frequently occur in MPA are in general directed against myeloperoxidase (MPO-ANCA). ANCA detected by IIF are also apparent in several other inflammatory conditions; in these cases, ANCA as detected by IIF is not specific for vasculitis. Therefore, ANCA should be demonstrated by using a combination of IIF and ELISA (1, 2).

The major problem with the current application of ANCA ELISA systems is the lack of international standard sera and the lack of international standardization of assay systems. Unfortunately, commercially available ELISA systems have a wide range of performance characteristics and employ arbitrary units determined by each manufacturer (3). When interpreting an ANCA test, therefore, the clinician must take into account the differences between the ELISA systems.

In Japan, three kinds of MPO-ANCA and PR3-ANCA ELISA systems are currently available as extracorporeal diagnostic agents authorized by the Ministry of Health and Welfare of Japan. Comparison of these ELISA systems with those commonly used in Europe is essential for international collaboration and for epidemiological and clinical research.

In the present study we compared the sensitivity and specificity of two major commercially available ANCA ELISA systems in Japan and one of the most widely used systems in Europe for MPO-ANCA and PR3-ANCA using plasma obtained from Japanese patients with a clinical and histological diagnosis of WG, MPA, or CSS. We also assessed the correlation of ANCA values among ELISA systems. This study aims to further validate the role of ANCA assays available in Japan and permit comparative international studies involving Japanese patients with AAV.

Patients and methods

Patient population and diagnostic criteria

The plasma samples were derived from newly diagnosed patients with primary systemic vasculitis (PSV) including WG, MPA, or CSS in accordance with the American College of Rheumatology (ACR) classification criteria and Chapel Hill consensus criteria (CHCC) with reference of EMEA algorithm method (4-7). We modified the algorithm to be irrespective of positivity of ANCA for the purpose of this study. 64 consecutive patients who had newly diagnosed disease were enrolled (MPA, n=52; CSS, n=1; WG, n=11) in the Department of Nephrology and Cardiovascular Medicine at Kyoto University hospital (Kyoto, Japan) between June 1999 and June 2000, in the Department of Nephrology and Dialysis and in the Department of Clinical Immunology and Rheumatology in Tazuke Kofukai Medical Research Institute Kitano Hospital (Osaka, Japan) between July 2000 and Apr 2008, and in the Department of Internal Medicine and Rheumatology in Juntendo University Hospital (Tokyo, Japan) between January 2005 and January 2006. The same number of plasma samples (n=58) were obtained during the untreated phase when the patients showed an acute exacerbation of symptom of organ involvement consistent with active vasculitis before the start of any immunosuppressive treatment. All patients had active disease at enrollment defined as Birmingham Vasculitis Activity Score (BVAS) of at least 4 (8). Plasma samples were also obtained from these patients in the follow up period between one week and six months after the start of immunosuppressive treatment (MPA, n=80; WG, n=2). All the patients were systematically assessed for potential subclinical granulomatous disease with diagnostic

imaging as well as ENT consultation. Confirmatory organ histological biopsies were available in eight out of 11 patients with WG including four renal biopsies, two lung biopsies, and two biopsies from nodules of paranasal sinuses. Renal biopsies were performed in all the MPA and CSS patients and revealed that all of them showed renal involvement.

For disease controls, we also assayed plasma from 64 consecutive new patients with non-vasculitic glomerulonephritis who had a renal biopsy in Kitano Hospital in this study period; diagnoses included IgA nephropathy (n=18), non-IgA type mesangioproliferative glomerulonephritis (n=5), endocapillary glomerulonephritis (n=1), interstitial nephritis (n=2), hepatitis C virus-related nephritis (n=1), membranoproliferative glomerulonephritis (n=3), membranous nephropathy (n=4), focal glomerulosclerosis (n=2), minimal change nephrotic syndrome (n=3), diabetic nephropathy (n=2), amyloidosis (n=1), malignant hypertension (n=1), nephrosclerosis (n=3), pseudo-Bartter syndrome (n=1), antiphospholipid syndrome (n=1), and lupus nephritis (n=6). None of the disease control patients were receiving immunosuppressive therapy at the time of sampling.

As healthy controls, the plasma samples from 55 people who received regular physical checkup in the clinic of Louis Pasteur Centre for Medical Research and had not have any diseases until 2004 were enrolled in this study.

This study was carried out in accordance with the 1975 Declaration of Helsinki of the World Medical Association. The design of the work has been approved by the ethical committee of the hospitals and clinic involved and each patient gave written informed consent for participation in the study.

All plasma samples were fully spun down to remove fibrin clots preventing non-specific reaction and were stored at -80°C until tested.

Methods of ANCA detection

All assays for MPO-, PR3-ANCA, and IIF were performed according to the manufacturers' instructions.

Nipro MPO- and PR3-ANCA ELISA. Nipro Nephroscholar MPO-ANC II kit (Nipro, Osaka, Japan; authorization number of diagnostic drugs and medications in Japan No. 212000AMZ00598000) has been developed in Japan. Briefly, The 1:500 diluted samples and biotinylated MPO antigen solution (0.1 mg/well) were applied onto the plate coated with Streptavidine and incubated for 1 hour at room temperature. The binding of MPO-ANCA to MPO antigens purified from human sputum was assessed using alkaline phosphatase (AP)-labeled polyclonal goat anti-human IgG with p-Nitrophenyl phosphate disodium in diethanolamine as a substrate. After adding sodium hydrate as stop solution, the absorbance was measured photometrically at 405 nm. The cut-off value was 20 ELISA Unit/ml.

Nipro Nephroscholar PR3-ANC kit (authorization No. 21000AMY00275000) is imported from Euro-Diagnostica (Arnhem, The Netherlands and Malmö, Sweden) and the kit is equivalent to Immunoscan PR3-ANCA (Euro-Diagnostica). Purified PR3 from human neutrophils were directly coated onto a 96-well microplate. The 1:50 diluted samples were applied onto the plate coated with purified PR3. AP-labeled polyclonal pig anti-human IgG was added followed by p-Nitrophenyl phosphate disodium in diethanolamine as a substrate. The absorbance was measured photometrically at 405 nm. The cut-off value was 10 ELISA Unit/ml.

MBL MPO- and PR3-ANCA ELISA. MBL (Nagoya, Japan) has imported the kits from Binding Site (Birmingham, UK). MBL MPO-ANCA test (BS) Code No.BS-031 (Nagoya, Japan; authorization No. 21100AMY00184000) is equivalent to BINDAZYME™ Human Anti-MPO Enzyme Immunoassay kit, Code No.MK031 (Binding Site). MBL PR3-ANCA test (BS) Code No.BS-032 (authorization No. 21000AMY00075000) is equivalent to BINDAZYME™ Human Anti-PR3 Enzyme Immunoassay kit, Code No.MK032 (Binding Site). Each sample, diluted 1:101 in diluent was used. The binding of MPO- and PR3-ANCA to human purified antigens coated on the plate was assessed using anti-human IgG peroxidase conjugate and 3, 3', 5, 5'-tetramethylbenzidine (TMB) as a chromogen. The absorbance was measured photometrically at 450 nm and the cut-off values for MPO- and PR3-ANCA were 9.0 U/ml and 3.5 U/ml, respectively.

Wieslab MPO-ANCA and Capture PR3-ANCA ELISA. These kits were not permitted for diagnostic purpose in Japan as of Apr 2008. For detection of MPO-ANCA by direct ELISA, Wielisa MPO-ANCA MPO 103 (Wieslab AB, Lund, Sweden) was used. MPO purified from human neutrophils was coated on 96-well plates. Samples were diluted at 1:80 and antibody binding was assessed with AP-conjugated anti-human IgG. Values >25 units were considered to be positive.

Capture PR3-ANCA testing was performed with Wielisa capture PR3-ANCA, Cap-PR3 108X. Each sample, diluted 1:80 in PBS was used. The antigen-antibody complex was detected by AP-labeled anti-human IgG antibodies using p-nitrophenylphosphate as a chromogen with spectrophotometric reading at 405 nm. For this method,the cut-off value was 25 U/ml.

Indirect immunofluorescence (IIF) assay. ANCA detection by IIF was performed on commercially available slides of ethanol-fixed and formalin-fixed purified normal granulocytes. The MBL Fluoro ANCA test Code No.4710 and 4720 (MBL) are equivalent to the Binding Site ANCA ethanol kit Code FK016 and ANCA formalin kit Code FK017 (Binding Site), respectively. If peri-nuclear or nuclear immunofluorescence was detected on ethanol-fixed granulocyte, the IIF was repeated using formalin-fixed neutrophil preparations. Samples were interpreted as P-ANCA positive if they displayed cytoplasmic staining on formalin-fixed slides. Plasma sample of untreated PSV patients (n=64), disease controls (n=54), and healthy controls (n=55) were tested for positivity of IIF-ANCA.

Statistics

Performance characteristics were compared by receiver operating characteristic (ROC) curve analysis according to the method described by Hanley (9).

Table I. Sensitivity and Specificity of MPO-ANCA for MPA using clinical cut off value of each ELISA systems.

ELISA kit		Sensitivity	Specificity	AUC	AUC	*P* versus		
	Cut off	(% [95%CI])	(% [95%CI])	(± SE)	95% CI	Nipro	MBL	Wieslab
Nipro MPO-ANCA	20 U/ml	90.4 [79.0 - 96.8]	98.2 [93.5 - 99.7]	0.946 ± 0.022	0.899 - 0.976		0.282	0.269
MBL MPO-ANCA	9 U/ml	88.2 [76.1 - 95.5]	96.3 [90.9 - 99.0]	0.970 ± 0.017	0.930 - 0.990	0.282		0.951
Wieslab MPO-ANCA	25 U/ml	86.5 [74.2 - 94.4]	99.1 [95.0 - 99.8]	0.971 ± 0.017	0.932 - 0.991	0.269	0.951	

MPA: microscopic polyangiitis; ROC: receiver operating characteristics curve analysis; AUC: area under the ROC curve; SE: standard error; 95% CI: 95% confidence interval.
Sample size: MPA, n=52; disease controls, n=54; and healthy controls n=55.

Table II. Sensitivity and Specificity of PR3-ANCA for WG using clinical cut off value of each ELISA systems.

ELISA kit		Sensitivity	Specificity	AUC	AUC	*P* versus		
	Cut off	(% [95%CI])	(% [95%CI])	(± SE)	95% CI	Nipro	MBL	Wieslab
Nipro PR3-ANCA	10 U/ml	100.0 [71.3 - 100.0]	98.2 [93.5 - 99.7]	0.986 ± 0.025	0.945- 0.998		0.729	0.211
MBL PR3-ANCA	3.5 U/ml	100.0 [71.3 - 100.0]	95.4 [88.4 – 97.9]	0.993 ± 0.017	0.957 - 0.998	0.729		0.163
Wieslab PR3 ANCA	25 U/ml	90.9 [58.7 – 98.5]	99.1 [95.0 – 99.8]	0.916 ± 0.059	0.851 - 0.959	0.211	0.163	

WG: Wegener's granulomatosis; ROC: receiver operating characteristics curve analysis; AUC: area under the ROC curve; SE, standard error; 95% CI: 95% confidence interval.
Sample size: WG, n=11; disease controls, n=54; and healthy controls, n=55.

A difference of $p<0.05$ was considered to be statistically significant. The Software MedCalc® version 9.3.0.0. (MedCalc®, Mariakerke, Belgium) was used for statistical analysis. A correlation coefficient between MPO-ANCA ELISA kits was obtained using Statview-J software version 5.0 for Windows (SAS Institute Inc., Cary, NC). A probability value <0.05 was considered significant.

Results

Clinical diagnostic performance of MPO-ANCA for MPA

Table I shows the sensitivity and specificity of MPO-ANCA for the diagnosis of MPA using predetermined cut-off values of each ELISA system. Plasma samples from untreated MPA patients (n=52), disease controls (n=54) and healthy controls (n=55) were used in this study. The sensitivity and specificity were 90.4% and 98.2% (Nipro), 88.2% and 96.3% (MBL), and 86.5% and 99.1% (Wieslab) (Table I).

ROC analysis and AUC, MPO-ANCA for MPA

ROC was analysed with plasma samples from patients with untreated MPA patients (n=52), disease controls (n=54), and healthy control (n=55). The overall diagnostic performance, assessed as the area under curve (AUC) of the four MPO-ANCA ELISAs were 0.946±0.022 (Nipro), 0.970±0.017 (MBL), and 0.971±0.017 (Wieslab). There were no significant differences among these ELISAs using pairwise comparison of ROC curves (Table I).

Clinical diagnostic performance of PR3-ANCA for WG

Table II shows the sensitivity and specificity of PR3-ANCA for the diagnosis of WG using predetermined cut-off values of each ELISA system. Plasma samples from untreated WG patients (n=11), disease controls (n=54), and healthy controls (n=55) were used in this study. The sensitivity and specificity were 100.0% and 98.2% (Nipro), 100.0% and 95.4% (MBL), and 90.9% and 99.1% (Wieslab) (Table II).

ROC analysis and AUC, PR3-ANCA for WG

ROC was analysed with plasma samples from untreated WG patients (n=11), disease controls (n=54), and healthy control (n=55). The AUC of PR3-ANCA ELISAs were 0.986±0.025 (Nipro), 0.993±0.017 (MBL), and 0.916±0.059 (Wieslab). There were no significant differences among these ELISAs using pairwise comparison of ROC curves (Table II).

Correlation between MPO-ANCA ELISA systems

Correlations between MPO-ANCA ELISAs were analysed using 146 plasma samples from patients with PSV at various stages (MPA, n=132; CSS, n=1; WG, n=13). All data were $\log_{10}$ transformed to normalise distributions prior to this analyses. Nipro MPO-ANCA ELISA was positively correlated with MBL MPO-ANCA ($r=0.891$, $p<0.0001$, Fig. 1) and Wieslab MPO-ANCA ($r=0.879$, $p<0.0001$). MBL MPO-ANCA and Wieslab MPO-ANCA were positively correlated with each other ($r=0.899$, $p<0.0001$, Table III).

Percentage of ANCA positivity in patients with PSV

MPO-ANCA positivity in MPA was 86.5% (45/52) in Nipro ELISA, 80.8% (42/52) in MBL ELISA, and 82.7% (43/52) in Wieslab ELISA. PR3-ANCA positivity in MPA was 3.8% (2/52) both in Nipro and Wieslab ELISAs, and 7.7 % (4/52) in MBL ELISAs. Absence of ANCA in MPA was 7.7 % (4/52) both in Nipro and MBL ELISAs, and 9.6% (5/52) in Wieslab ELISA. PR3-ANCA positivity in WG was 100% (11/11) both in Nipro and MBL ELISAs, and 90.9% (10/11) in Wieslab ELISA. A CSS patient showed positive MPO-ANCA only in MBL ELISA (Table IV).

Table III. Correlation coefficient between MPO-ANCA ELISAs.

MPO-ANCA ELISAs	Nipro	MBL [BS]	Wieslab
Nipro	–	0.891	0.879
MBL	0.891	–	0.899
Wieslab	0.879	0.899	–

Samples with PSV before treatment and in the follow up period (n=146).

Table IV. Percentage of ANCA positivity in PSV patients.

	Diagnosis / ELISA positivity	MPA % (n)	WG % (n)	CSS % (n)
Nipro	MPO-ANCA	86.5 (45/52)	0 (0/11)	0 (0/1)
	PR3-ANCA	3.8 (2/52)	100.0 (11/11)	0 (0/1)
	Double positive	1.9 (1/52)	0 (0/11)	0 (0/1)
	Double negative	7.7 (4/52)	0 (0/11)	100.0 (1/1)
MBL	MPO-ANCA	80.8 (42/52)	0 (0/11)	100.0 (1/1)
	PR3-ANCA	7.7 (4/52)	100.0 (11/11)	0 (0/1)
	Double positive	3.8 (2/52)	0 (0/11)	0 (0/1)
	Double negative	7.7 (4/52)	0 (0/11)	0 (0/1)
Wieslab	MPO-ANCA	82.7 (43/52)	0 (0/11)	0 (0/1)
	PR3-ANCA	3.8 (2/52)	90.9 (10/11)	0 (0/1)
	Double positive	3.8 (2/52)	0 (0/11)	0 (0/1)
	Double negative	9.6 (5/52)	9.1 (1/11)	100.0 (1/1)

Double positive, both MPO- and PR3-ANCA positive;
Double negative, both MPO- and PR3-ANCA negative;
MPA: microscopic polyangiitis; WG: Wegener's granulomatosis;
CSS: Churg-Strauss syndrome.

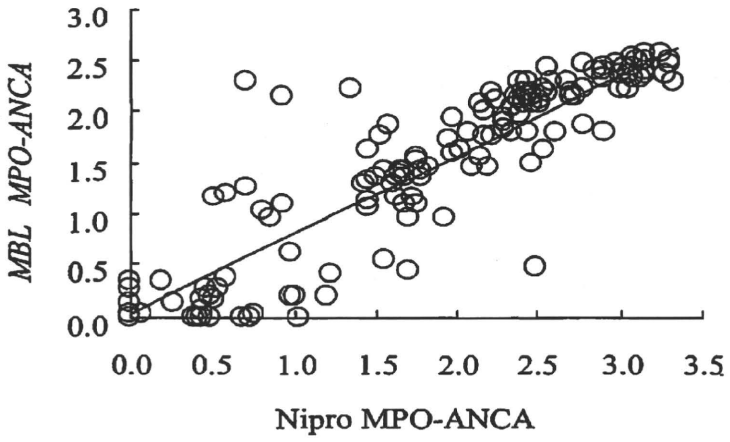

Fig. 1. *Correlation between Nipro MPO-ANCA and MBL MPO-ANCA.* Correlations between MPO-ANCA were analysed using 146 plasma samples from patients with PSV in the active and follow-up stages (MPA, n=132; CSS, n=1; WG, n=13). Nipro MPO-ANCA and MBL MPO-ANCA positively correlated with each other ($r = 0.891$, $p<0.0001$). *Estimated Nipro MPO-ANCA* = 1.0146×MBL MPO-ANCA + 0.3545, *Estimated MBL MPO-ANCA* = 0.7829 ×Nipro MPO-ANC II + 0.0265. All data were $\log_{10}$ transformed to normalise distributions prior to these analyses.

Clinical diagnostic performance of IIF for PSV.

Plasma samples of untreated PSV patients (n=64), disease controls (n=54), and healthy controls (n=55) were tested for positivity of IIF-ANCA. IIF showed a sensitivity of 81.3% (95% CI, 69.5–89.9) and 94.5% specificity (88.4–97.9) for active PSV.

P-ANCA and C-ANCA were detected in 46 and 11 out of the total 173 samples. Among the 57 samples with positive P- or C-ANCA by IIF, 56 samples were positive for MPO- and/or PR3-ANCA by Nipro MPO- and PR3-ANCA ELISAs. All the 57 samples with positive P- or C-ANCA were positive for MPO- and/or PR3-ANCA by MBL MPO- and PR3-ANCA ELISAs. The result of ELISAs by Nipro and MBL were well corresponded with ANCA by IIF. P-ANCA positivity in MPA was 82.7% (43/52), while C-ANCA positivity in MPA was 7.7% (4/52). Absence of P- and C-ANCA in MPA was 9.6% (5/52). C-ANCA and P-ANCA positivity in WG is 54.5% (6/11) and 9.1% (1/11) respectively. Absence of P- and C-ANCA in WG was 36.4% (4/11). IIF-ANCA was negative in our CSS patient (Table V).

Discussion

In this study we investigated ANCA ELISA systems authorized by the Japanese Ministry of Health and Welfare for diagnostic purpose: a streptavidin coated capture ELISA and a direct ELISA for MPO-ANCA and direct ELISAs for PR3-ANCA.

The present study shows that the ELISA systems widely used in Japan are highly sensitive and specific for detection of MPO-ANCA in MPA. There were no detectable differences in diagnostic performance between ELISA systems as analysed by ROC curve analysis.

The incidence of WG among the ANCA-associated systemic vasculitides is higher than MPA in northern Europe (10-13). By contrast, nationwide Japanese surveys demonstrated that the prevalence of patients with WG is very low compared with that of patients with MPA (14). Fujimoto *et al.* shows that the estimated annual incidence of MPA in Miyazaki Prefecture, the Southern part of Japan, is 14.8/million, which is as frequent as that of ANCA-associated systemic vasculitides identified in several European studies. They also demonstrate that MPA are more common than WG among the ANCA-associated vasculitides in Japan (15). MPO-ANCA was identified in 79 to 93% of patients with MPA in Japan, whereas reports from Europe described the ratio as being 44 to 69% (12-19).

Table V. Percentage of indirect immunofluorescence (IIF) test positivity in primary systemic vasculitis patients.

Diagnosis IIF positivity	MPA % (n)	WG % (n)	CSS % (n)
P-ANCA	82.7 (43/52)	9.1 (1/11)	0 (0/1)
C-ANCA	7.7 (4/52)	54.5 (6/11)	0 (0/1)
Negative	9.6 (5/52)	36.4 (4/11)	100 (1/1)

P-ANCA: perinuclear ANCA; C-ANCA: cytoplasmic ANCA;
Negative: both P- and C-ANCA negative.

Although differences in several clinico-epidemiological manifestations among vasculitides have been identified between Japan and European countries, it was suspected that such difference may result from different ELISA systems employed in Japan and Europe. However, this study shows MPO-ANCA predominance in Japan is not due to the different ELISA system employed in Japan and Europe. Therefore, the ANCA-associated systemic vasculitides epidemiologically and serologically differ between Japan and European countries.

Nevertheless, we should still bear in mind that there are significant differences in sensitivity and specificity among commercially available ELISA systems (3, 20-25). The reason might be that in ELISAs, proteins are denatured during antigen purification or coating onto the solid phase, thereby hiding or destroying conformational epitopes on PR3 or MPO. In order to avoid this, capture ELISA in which the plate is pre-coated with a monoclonal antibody to capture the antigen has been designed. Csernok *et al.* reported that capture PR3 ELISA was a highly sensitive assay in WG in several international laboratories (23). Recently Hellmich *et al.* reported sensitivity of a new anchor PR3-ELISA for WG was superior to those of usual direct or capture PR3-ELISA. They used a new technique to immobilize PR3 on the ELISA plate by using a bridging molecule as an "anchor" preventing direct adhesion to the plastic surface and thereby preserving all epitopes for binding with ANCA (24).

Another important issue is that the lack of the standard sera and international unit makes it difficult to compare ELISAs from different manufacturers. For example, Nipro MPO-ANCA and MBL MPO-ANCA are widely used in reference laboratories or university hospitals in Japan. Although sensitivity and specificity were not different between these two systems and they were positively correlated with each other (Fig. 1, Table III), the absolute values obtained from these two ELISA systems cannot be compared because they do not use the same standard serum.

We should also discuss cut-off values employed in the ELISA systems. Holle *et al.* analysed ANCA ELISAs from 11 manufacturers and reported that applying the manufacturers' cut off values results in great variation in sensitivity. Lowering the cut off values increased the sensitivity and reduced specificity but increased overall diagnostic performance (3). They concluded that the low sensitivity of some commercial ELISA systems reflects the high cut off values rather than methodological problems in the assays.

For standardization of ANCA testing, the BCR office of the European Union sponsored a large international standardization project of monitoring different antigen purification methods (26), suitability of purified antigens for solid-phase assays and standardization (27), and clinical utility of the developed tests (28). In the meantime, before the results become clear, it is important that laboratories should understand the difference and limitations of the assays in use.

A limitation of our study is the small number of WG samples. It was difficult to collect samples from patients with active and untreated WG because MPA with renal involvement predominates in Japan but we do not see patients with WG presenting to renal units. Therefore the PR3-ANCA ELISA kit available in Japan is not manufactured in Japan. Nipro PR3-ANCA is equivalent to Immunoscan PR3-ANCA (Euro-Diagnostica) and MBL PR3-ANCA is equivalent to BINDAZYME™ Human Anti-PR3 Enzyme Immunoassay kit (Binding Site). These kits are used internationally and already well screened in the world. Trevisin *et al.* reported that sensitivity of Euro-Diagnostica Immunoscan PR3-ANCA was 90% sensitivity and 96% specificity (25). Binding Site BINDAZYME RP3-ANCA ELISA were reported 60-96% sensitivity and 88-100% specificity. (3, 25, 29). Further study should be required to investigate the performance of the ELISA systems using larger samples from Japanese patients with active and untreated WG. Then, it would be possible to more directly compare the performance of ELISAs for WG between Europe and Japan.

Another limitation is that we used plasma and not serum samples. However, Lee *et al.* reported that ANCA positivity between serum and plasma as measured by commercially available ELISA systems was concordant, and that ANCA levels in serum and plasma measured by solid phase assays correlated well (30). Therefore, our results could be compared with those tested with serum samples.

In summary, the two major MPO-ANCA ELISA systems commercially available in Japan exhibited high sensitivity and specificity that provided similar diagnostic value with the ELISA systems used in Europe. Thus, the results of ANCA testing in Japan may be compared to those from other countries. This will facilitate future international surveys exploring differences in the epidemiology of PSV, and aetiological factors contributing to their pathogenesis.

Acknowledgements

The authors thank Dr. Katsumi Yagi, Louis Pasteur Center for Medical Research, for advices in statistical analysis and Dr. Masato Yagita, Department of Clinical Immunology and Rheumatology, Tazuke Kofukai Medical Research Institute, Kitano Hospital, for providing patient blood samples for analysis.

References

1. SAVIGE J, GILLIS D, BENSON E *et al.*: International Consensus Statement on Testing and Reporting of Antineutrophil Cytoplasmic Antibodies (ANCA). *Am J Clin Pathol* 1999; 111: 507-13.
2. SAVIGE J, DIMECH W, FRITZLER M *et al.*: Addendum to the International Consensus Statement on testing and reporting of antineutrophil cytoplasmic antibodies. Quality control guidelines, comments, and recommendations for testing in other autoimmune diseases. *Am J Clin Pathol* 2003; 120: 312-8.
3. HOLLE JU, HELLMICH B, BACKES M *et al.*: Variations in performance characteristics of commercial enzyme immunoassay kits for detection of antineutrophil cytoplasmic antibodies: what is the optimal cut off? *Ann Rheum Dis* 2005; 64: 1773-9.
4. LEAVITT RY, FAUCI AS, BLOCH DA *et al.*: The American College of Rheumatology 1990 criteria for the classification of Wegener's granulomatosis. *Arthritis Rheum* 1990; 33: 1101-7.
5. MASI AT, HUNDER GG, LIE JT *et al.*: The American College of Rheumatology 1990 criteria for the classification of Churg-Strauss syndrome (allergic granulomatosis and angiitis). *Arthritis Rheum* 1990; 33: 1094-100.
6. JENNETTE JC, FALK RJ, ANDRASSY K *et al.*: Nomenclature of systemic vasculitides. Proposal of an international consensus conference. *Arthritis Rheum* 1994; 37: 187-92.
7. WATTS R, LANE S, HANSLIK T *et al.*: Development and validation of a consensus methodology for the classification of the ANCA-associated vasculitides and polyarteritis nodosa for epidemiological studies. *Ann Rheum Dis* 2007; 66: 222-7.
8. LUQMANI RA, BACON PA, MOOTS RJ *et al.*: Birmingham Vasculitis Activity Score (BVAS) in systemic necrotizing vasculitis. *QJM* 1994; 87: 671-8.
9. HANLEY JA, MCNEIL BJ: The meaning and use of the area under a receiver operating characteristic (ROC) curve. *Radiology* 1982; 143: 29-36.
10. HAUGEBERG G, BIE R, BENDVOLD A *et al.*: Primary vasculitis in a Norwegian community hospital: a retrospective study. *Clin Rheumatol* 1998; 17: 364-8.
11. WATTS RA, LANE SE, BENTHAM G *et al.*: Epidemiology of systemic vasculitis: a ten-year study in the United Kingdom. *Arthritis Rheum* 2000; 43: 414-9.
12. LANE SE, SCOTT DG, HEATON A *et al.*: Primary renal vasculitis in Norfolk-increasing incidence or increasing recognition? *Nephrol Dial Transplant* 2000; 15: 23-7.
13. REINHOLD-KELLER E, HERLYN K, WAGNER-BASTMEYER R *et al.*: Stable incidence of primary systemic vasculitides over five years: Results from German vasculitis register. *Arthritis Rheum* 2005; 53: 93-9.
14. SAKAI H, KUROKAWA K, KOYAMA A *et al.*: [Guidelines for the management of rapidly progressive glomerulonephritis] *Nippon Jinzo Gakkai Shi* 2002; 44: 55-82.(in Japanese)
15. FUJIMOTO S, UEZONO S, HISANAGA S *et al.*: Incidence of ANCA-associated primary renal vasculitis in the Miyazaki prefecture: the first population-based retrospective, epidemiologic survey in Japan. *Clin J Am Soc Nephrol* 2006; 1: 1016-22.
16. GONZALEZ-GAY MA, GARCIA-PORRUA C, GUERRERO J *et al.*: The epidemiology of the systemic vasculitides in northwest Spain: Implications of the Chapel Hill Consensus Conference Definitions. *Arthritis Rheum* 2003; 49: 388-93.
17. TIDMAN M, OLANDER R, SVALANDER C *et al.*: Patients hospitalized because of small vessel vasculitides with renal involvement in the period 1975-1995: organ involvement, ANCA patterns, seasonal attack rates and fluctuation of annual frequencies. *J Intern Med* 1998; 244: 133-41.
18. HAUER HA, BAJEMA IM, VAN HOUWELINGEN HC *et al.*: Renal histology in ANCA-associated vasculitis: Differences between diagnostic and serologic subgroups. *Kidney Int* 2002; 61: 80-9.
19. FRANSSEN CF, STEGEMAN CA, KALLENBERG CG *et al.*: Antiproteinase 3- and antimyeloperoxidase-associated vasculitis. *Kidney Int.* 2000; 57: 2195-206.
20. SPECKS U, WIEGERT EM, HOMBURGER HA: Human mast cells expressing recombinant proteinase 3 (PR3) as substrate for clinical testing for anti-neutrophil cytoplasmic antibodies (ANCA). *Clin Exp Immunol* 1997; 109: 286-95.
21. LIM LC, TAYLOR JG 3RD, SCHMITZ JL *et al.*: Diagnostic usefulness of antineutrophil cytoplasmic autoantibody serology. Comparative evaluation of commercial indirect fluorescent antibody kits and enzyme immunoassay kits. *Am J Clin Pathol* 1999; 111: 363-9.
22. CSERNOK E, AHLQUIST D, ULLRICH S *et al.*: A critical evaluation of commercial immunoassays for antineutrophil cytoplasmic antibodies directed against proteinase 3 and myeloperoxidase in Wegener's granulomatosis and microscopic polyangiitis. *Rheumatology* (Oxford) 2002; 41: 1313-7.
23. CSERNOK E, HOLLE J, HELLMICH B *et al.*: Evaluation of capture ELISA for detection of antineutrophil cytoplasmic antibodies directed against proteinase 3 in Wegener's granulomatosis: first results from a multicentre study. *Rheumatology* (Oxford) 2004; 43: 174-80.
24. HELLMICH B, CSERNOK E, FREDENHAGEN G *et al.*: A novel high sensitivity ELISA for detection of antineutrophil cytoplasm antibodies against proteinase-3. *Clin Exp Rheumatol* 2007; 25: S1-5.
25. TREVISIN M, POLLOCK W, DIMECH W *et al.*: Antigen-Specific ANCA ELISAs Have Different Sensitivities for Active and Treated Vasculitis and for Nonvasculitic Disease. *Am J Clin Pathol* 2008; 129: 42-53.
26. HAGEN EC, ANDRASSY K, CHERNOK E *et al.*: The value of indirect immunofluorescence and solid phase techniques for ANCA detection. A report on the first phase of an international cooperative study on the standardization of ANCA assays. EEC/BCR Group for ANCA Assay Standardization. *J Immunol Methods* 1993; 159: 1-16.
27. HAGEN EC, ANDRASSY K, CSERNOK E *et al.*: Development and standardization of solid phase assays for the detection of anti-neutrophil cytoplasmic antibodies (ANCA). A report on the second phase of an international cooperative study on the standardization of ANCA assays. *J Immunol Methods* 1996; 196: 1-15.
28. HAGEN EC, DAHA MR, HERMANS J *et al.*: Diagnostic value of standardized assays for anti-neutrophil cytoplasmic antibodies in idiopathic systemic vasculitis. EC/BCR Project for ANCA Assay Standardization. *Kidney Int* 1998; 53: 743-53.
29. POLLOCK W, DUNSTER K, ROLLAND JM *et al.*: A comparison of commercial and in-house ELISAs for antineutrophil cytoplasmic antibodies directed against proteinase 3 and myeloperoxidase. *Pathology* 1999; 31: 38-43.
30. LEE AS, FINKIELMAN JD, PEIKERT T *et al.*: Agreement of anti-neutrophil cytoplasmic antibody measurements obtained from serum and plasma. *Clin Exp Immunol* 2006; 146: 15-20.

Acute Renal Failure After Exercise in a Japanese Sumo Wrestler With Renal Hypouricemia

AKIRA MIMA, MD, PHD; KIMIYOSHI ICHIDA, MD, PHD; TAKESHI MATSUBARA, MD, PHD; HIROSHI KANAMORI, MD; EMI INUI, MD; MISA TANAKA, MD, PHD; YUMI MANABE, MD; NORIYUKI IEHARA, MD, PHD; YOSHINORI TANAKA, MD; MOTOKO YANAGITA, MD, PHD; ATSUKO YOSHIOKA, MD; HIDENORI ARAI, MD, PHD; MASASHI KAWAMURA, MD; KATSUMASA USAMI, MD; TATSUO HOSOYA, MD, PHD; TORU KITA, MD, PHD; ATSUSHI FUKATSU, MD, PHD

ABSTRACT: Familial renal hypouricemia is a hereditary disease characterized by extraordinary high renal uric acid clearance and is associated with acute renal failure (ARF). An 18-year-old sumo wrestler developed ARF after anaerobic exercise. Several hours after the exercise, he had a pain in the loins with oliguria, headache, and nausea. On admission, his serum uric acid was decreased despite the elevation of serum creatinine (9.5 mg/dL). The level of creatine kinase was normal and there was no myoglobinuria or urolithiasis. Magnetic resonance imaging showed no significant abnormality. Renal function improved completely within 2 weeks of hydration treatment. After remission, hypouricemia became obvious (1.0 mg/dL) from the initial level of uric acid (6.1 mg/dL) and fractional excretion of uric acid was 49%. Polymerase chain reaction of a urate anion exchanger known to regulate blood urate level (*SLC22A12* gene: *URAT1*) demonstrated that homozygous mutations in exon 4 (W258X). Both parents showed heterozygous mutation of the *URAT1* gene, but both siblings showed no mutation. Thus, we describe a Japanese sumo wrestler of familial renal hypouricemia complicated with anaerobic exercise-induced ARF, with definite demonstration of genetic abnormality in the responsible gene, *URAT1*. **KEY INDEXING TERMS:** Renal hypouricemia; Acute renal failure; *URAT1* gene. **[Am J Med Sci 2008; 336(6):512–514.]**

Hypouricemia, defined as low levels of serum urate (less than 2.0 mg/dL), has been recognized as a predisposition toward exercise-induced acute renal failure (ARF). The incidence of hypouricemia is reported to be 0.16% in men and 0.23% in women among normal adults,[1] and to be 2.54% in hospitalized patients.[2] Exercise-induced ARF has been increasing, although hypouricemia is not a rare condition. Patients complain of severe loin pain with nausea and vomiting after anaerobic exercise.[3] Although some patients need to have dialysis because of ARF, short-term prognosis of these patients seems to be good.[4–7] Recently, patients with idiopathic renal hypouricemia are found to have mutations in the gene (*SLC22A12*) encoding for human urate transporter 1 (hURAT1), and several *URAT1* genetic mutations have been revealed in patients with hypouricemia.[8,9]

In this article, we report a Japanese sumo wrestler with anaerobic exercise-induced ARF associated with renal hypouricemia caused by a mutation in the *URAT1* gene.

Case Report

The patient is an 18-year-old Japanese sumo wrestler and his patients are healthy. He was born after normal pregnancy and delivery. He had no family history of ARF or any renal diseases. He was admitted to a hospital because of nausea, vomiting, headache, and severe loin pain after anaerobic exercise. On admission, serum BUN and creatinine were elevated to 74 mg/dL and 9.5 mg/dL, respectively, with a slight decrease in serum uric acid (6.1 mg/dL). The level of creatine kinase was normal and there was no myoglobinuria or urolithiasis. The urine output was 200 to 300 mL/day. After hydration therapy, he was transferred to our hospital for further examination. On admission to our hospital, his height and weight were 165 cm and 100 kg, respectively. He had no oliguria in our hospital. Physical examination revealed no abnormalities. Laboratory test of this patient showed a hemoglobin 15.0 g/dL, hematocrit 44.8%, leukocyte count 7100/μL with normal differentiation, platelet 217,000/μL, total protein 7.2 g /dL, serum sodium 143

From the Department of Nephrology (AM, TM, HK, EI, MT, YM, NI, YT, MY, AY, AF), Kyoto University Graduate School of Medicine, Kyoto, Japan; Division of Kidney and Hypertension, Department of Internal Medicine (KI, TH), Jikei University School of Medicine, Tokyo, Japan; Departments of Geriatric Medicine (HA) and Cardiovascular Medicine (TK), Kyoto University Graduate School of Medicine, Kyoto, Japan; Department of Internal Medicine (MK), Kochi Prefectural Hata Kenmin Hospital, Kochi, Japan; and Department of Internal Medicine (KU), Ijinkai Takeda General Hospital, Kyoto, Japan.

Submitted October 21, 2007; accepted in revised form November 28, 2007.

Correspondence: Akira Mima, M.D., Ph.D., Departments of Nephrology, Kyoto University Graduate School of Medicine, 54 Kawahara-cho, Shogoin, Sakyo-ku, Kyoto 606-8507, Japan (E-mail: amima@kuhp.kyoto-u.ac.jp).

Table 1. Laboratory Data of Family Members

	Serum Uric Acid (S-UA) (mg/dL)	Urine Uric Acid (U-UA) (mg/dL)	Creatinine Clearance (Ccr) (mL/min)	FEUA (%)
Present case	1.0	44	116.4	52
Father	4.7	61.2	118.5	15.2
Mother	3.2	21.1	129.9	5.7
Sister	4.7	78	111.4	8.1
Paternal grandfather	4.7	20.5	53.5	5.8
Maternal grandfather	3.5	26	122.1	6.5

mEq/L, serum potassium 4.0 mEq/L, serum chloride 106 mEq/L, serum calcium 9.4 mg/dL, serum phosphate 3.9 mg/dL, serum BUN 12 mg/dL, serum creatinine 1.3 mg/dL, serum uric acid 1.0 mg/dL, bicarbonate 24.6 mmol/L, serum creatinine kinase 83 U/L, antistreptolysin O 232 IU/mL, and fractional excretion of sodium 0.59%. The following parameters were within normal limits or negative: total cholesterol, aspirate aminotransferase, alanine aminotransferase, lactate dehydrogenase, C-reactive protein, antinuclear antibody, serum hemolytic complement activity, hepatitis B surface antigen, hepatitis C antibody. On urinalysis glucosuria, aminoaciduria or crystallization was not found, and there were no other abnormal data observed, except significantly higher fractional excretion of uric acid (FEUA) (52%; normal 7%–12%). These results suggested that diagnosis of renal hypouricemia, not existing dysfunction of the proximal renal tubule leading excessive urinary losses of amino acids, glucose, bicarbonate, phosphate, and uric acid. Test with the pyrazinamide or probenecid, which are inhibitors of the renal urate transporting systems were not performed.

Electrocardiogram and X-ray films of chest and abdomen were normal. An abdominal magnetic resonance imaging scan did not reveal slight swollen kidney, but wedge-shaped images were not recognized.

Table 1 shows the laboratory examination data of the patient and his family members. The levels of serum uric acid and FEUA were within normal limits in his grandfathers, parents, and sister. The mutational analysis of the *SLC22A12* gene was performed after obtaining informed consent and revealed that he was homozygous for W258X. His grandfathers and parents were heterozygous for W258X, although his sister was wild type (Figures 1 and 2). We guided him to warm up before exercise. Although marked hypouricemia (0.8–1.0 mg/dL) has persisted, a similar ARF episode has not occurred.

Discussion

Hypouricemia is defined as serum uric acid concentrations lower or equal to 2 mg/dL.[10] It is a fairly common abnormality, which occurs in 0.5%–4.0% of general populations and occurs in about 1% of hospitalized patients .[2,11,12] It can be caused by reduced uric acid production or by reduced renal tubular reabsorption of filtered uric acid. The incidence of renal hypouricemia has been reported to fall in the range 0.12% to 0.72%.[13]

Renal hypouricemia is a hereditary condition of increased renal urate clearance caused by an isolated inborn error of membrane transport for urate in the renal proximal tubule. Recently, Enomoto et al[8] proposed a model of indirect coupling of sodium and urate transport and identified in the human

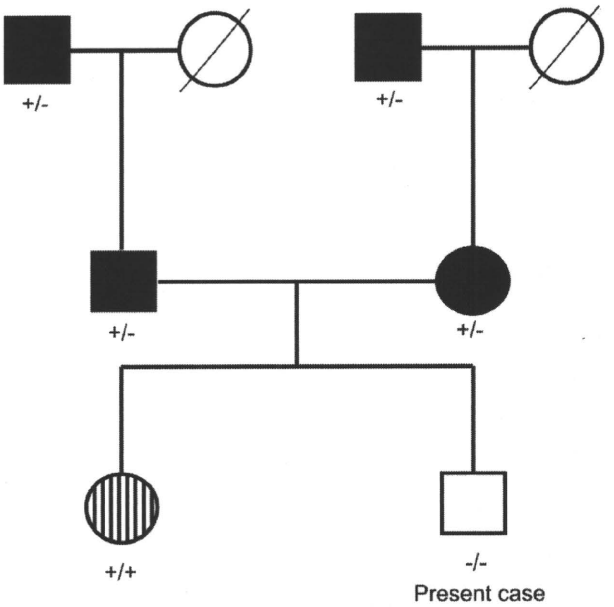

Figure 1. Mutations of *SLC22A12* (*URAT1*). Men are denoted by squares, women by circles. Clinical status is indicated as follows: typical clinical manifestations of hereditary renal hypouricemia (homozygous): thick open squares; heterozygous mutation: solid symbols; unaffected individual: hatched symbol.

kidney, URAT1, encoded by *SLC22A12*. Intracellular accumulation of sodium and urate for which URAT1 has affinity will favor the reabsorption of urate in exchange for anions, which move down their electromechanical gradients into the tubular lumen. Most patients with idiopathic renal hypouricemia have loss-of-function mutations in *SLC22A12*.[9] In this study, the parents of patient, who are heterozygous for W258X, had normal FEUA without hypouricemia. In contrast, the patient, a homozygous for W258X had much more severe hypouricemia with much higher FEUA than them.

Most mutations in *SLC22A12* have been detected in hypouricemic patients and the W258X mutation, which produces a nonfunctioning truncated protein that lacks half of the mature protein, is the predominant *SLC22A12* mutation,[8] and was detected in 40 of 54 mutated alleles. About half of those with *SLC22A12* mutations were homozygotes, about 30% were compound heterozygotes, and the rest were heterozygotes[8,9] As in this case, the serum uric acid level was lower than 1.0 mg/dL in almost all homozygotes and compound heterozygoutes.

Exercise-induced ARF with renal hypouricemia has typical clinical features; ARF can develop after acute anaerobic exercise in conjunction with severe loin pain, but without evidence of massive rhabdomyolysis.[4–7] Precise mechanisms of this nephropathy are still unknown, but one possibility is that an increase of oxygen free radicals produced during exercise leads to renal tissue

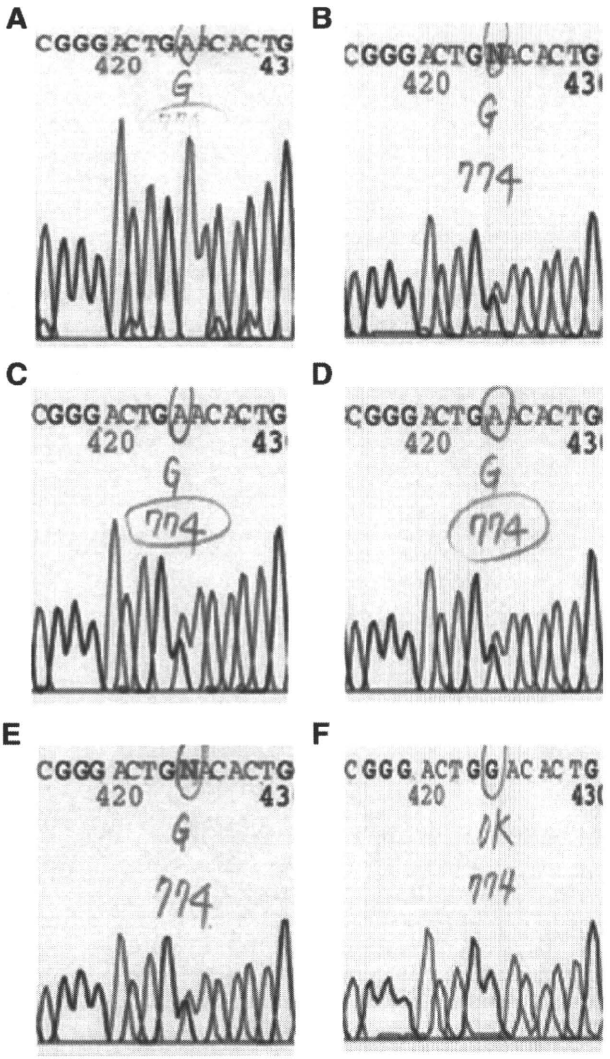

Figure 2. Partial sequencing data of the *SLC22A12* gene. (A) A homozygous G to A transition at nucleotide 774 in exon 4, which results in a codon change of W258X, in present case. (B) A heterozygous transition at nucleotide 774 (W258X) in patient's father. (C) A heterozygous G to A transition at nucleotide 774 (W258X) in patient's mother. (D) A heterozygous G to A transition at nucleotide 774 (W258X) in patient's paternal grandfather. (E) A heterozygous transition at nucleotide 774 (W258X) in patient's maternal grandfather. (F) A normal sequence in patient's sister.

damage.[14] Because uric acid seems to be a strong antioxidant and a scavenger of free radicals, that could spoil the renal function during anaerobic exercise.[14] Our sequence analysis of the *URAT1* gene of all family members showed that the patient had homozygous mutations in exon 4 (W258Stop), resulting in premature truncated URAT1 protein, whereas his grand fathers and parents showed heterozygous mutations. These phenomena led that healthy grand fathers and parents with the heterozygous *SLC22A12* mutation whose serum urate level and FEUA were in the normal range.

Although it is not known whether mutations in the *URAT1* gene can explain several types of a urate-transporting defect in renal hypouricemic patients such as so called four-component model (presecretory reabsorption defect, postsecretpry reabsorption defect, or hyper secretion defect). Moreover, patients with presecretory reabsorption defect do not always show exercise-induced ARF. Differences in mutations of the *URAT1* gene might be responsible for the difference in the clinical features. Further investigations will be needed to detect new mutations or to detect unknown urate transporter. Interestingly, Ichida et al have shown 8 new *SLC22A12* renal hypouricemia mutations.

In summary, we report a Japanese sumo wrestler who often takes anaerobic exercise-induced ARF associated with renal hypouricemia. Furthermore, it is recognized that he has a homozygous mutation of *SLC22A12*.

Acknowledgments

We thank Takako Pezzotti, Maki Watanabe, and Ayumi Hosotani (Kyoto University) for excellent technical assistance.

References

1. **Erley CM, Hirschberg RR, Hoefer W, et al.** Acute renal failure due to uric acid nephropathy in a patient with renal hypouricemia. Klin Wochenschr 1989;67:308–12.
2. **Ogino K, Hisatome I, Saitoh M, et al.** Clinical significance of hypouricemia in hospitalized patients. J Med 1991;22:76–82.
3. **Ohta T, Sakano T, Ogawa T, et al.** Exercise-induced acute renal failure with renal hypouricemia: a case report and a review of the literature. Clin Nephrol 2002;58:313–6.
4. **Ishikawa I.** Acute renal failure with severe loin pain and patchy renal ischemia after anaerobic exercise in patients with or without renal hypouricemia. Nephron 2002;91:559–70.
5. **Ishikawa I, Sakurai Y, Masuzaki S, et al.** Exercise-induced acute renal failure in 3 patients with renal hypouricemia. Nippon Jinzo Gakkai Shi 1990;32:923–8.
6. **Igarashi T, Sekine T, Sugimura H, et al.** Acute renal failure after exercise in a child with renal hypouricaemia. Pediatr Nephrol 1993;7:292–3.
7. **Hisanaga S, Kawamura M, Uchida T, et al.** Exercise-induced renal failure in a patient with hyperuricosuric hypouricemia. Nephron 1994;66:475–6.
8. **Enomoto A, Wempe MF, Tsuchida H, et al.** Molecular identification of a novel carnitine transporter specific to human testis. Insights into the mechanism of carnitine recognition. J Biol Chem 2002;277:36262–71.
9. **Ichida K, Hosoyamada M, Hisatome I, et al.** Clinical and molecular analysis of patients with renal hypouricemia in Japan-influence of URAT1 gene on urinary urate excretion. J Am Soc Nephrol 2004;15:164–73.
10. **Sperling O.** Renal hypouricemia: classification, tubular defect and clinical consequences. Contrib Nephrol 1992;100:1–14.
11. **Maesaka JK, Fishbane S.** Regulation of renal urate excretion: a critical review. Am J Kidney Dis 1998;32:917–33.
12. **Bairaktari ET, Kakafika AI, Pritsivelis N, et al.** Hypouricemia in individuals admitted to an inpatient hospital-based facility. Am J Kidney Dis 2003;41:1225–32.
13. **Hisatome I, Ogino K, Kotake H, et al.** Cause of persistent hypouricemia in outpatients. Nephron 1989;51:13–16.
14. **Ames BN, Cathcart R, Schwiers E, et al.** Uric acid provides an antioxidant defense in humans against oxidant- and radical-caused aging and cancer: a hypothesis. Proc Natl Acad Sci USA 1981;78:6858–62.

Expression of BMP-7 and USAG-1 (a BMP antagonist) in kidney development and injury

M Tanaka[1], S Endo[1], T Okuda[2], AN Economides[3], DM Valenzuela[3], AJ Murphy[3], E Robertson[4], T Sakurai[5], A Fukatsu[6], GD Yancopoulos[3], T Kita[1] and M Yanagita[2]

[1]Department of Cardiovascular Medicine, Graduate School of Medicine, Kyoto University, Kyoto, Japan; [2]COE Formation for Genomic Analysis of Disease Model Animals with Multiple Genetic Alterations, Graduate School of Medicine, Kyoto University, Kyoto, Japan; [3]Regeneron Pharmaceuticals Inc., Tarrytown, New York, USA; [4]Wellcome Trust Center for Human Genetics, University of Oxford, Oxford, UK; [5]Department of Pharmacology, Institute of Basic Medical Sciences, University of Tsukuba, Ibaraki, Japan and [6]Department of Artificial Kidneys, Graduate School of Medicine, Kyoto University, Kyoto, Japan

Once developed, end-stage renal disease cannot be reversed by any current therapy. Bone morphogenetic protein-7 (BMP-7), however, is a possible treatment for reversing end-stage renal disease. Previously, we showed that the BMP antagonist uterine sensitization-associated gene-1 (USAG-1, also known as ectodin and sclerostin domain-containing 1) negatively regulates the renoprotective action of BMP-7. Here, we show that the ratio between USAG-1 and BMP-7 expression increased dramatically in the later stage of kidney development, with USAG-1 expression overlapping BMP-7 only in differentiated distal tubules. Examination of USAG-1 expression in developing kidney indicated that a mosaic of proximal and distal tubule marker-positive cells reside side by side in the immature nephron. This suggests that each cell controls its own fate for becoming a proximal or distal tubule cell. In kidney injury models, the ratio of USAG-1 to BMP-7 expression decreased with kidney damage but increased after subsequent kidney regeneration. Our study suggests that USAG-1 expression in a kidney biopsy could be useful in predicting outcome.

Kidney International (2008) **73**, 181–191; doi:10.1038/sj.ki.5002626; published online 17 October 2007

KEYWORDS: kidney disease; differentiation; nephron segment

Correspondence: *M Yanagita, Graduate School of Medicine, Kyoto University, Yoshida-Konoe-cho, Kyoto, Japan 606-8501.*
E-mail: motoy@kuhp.kyoto-u.ac.jp

Received 6 April 2007; revised 3 August 2007; accepted 14 August 2007; published online 17 October 2007

Bone morphogenetic proteins (BMPs) are phylogenetically conserved signaling molecules that belong to the transforming growth factor-β superfamily.[1] Although these proteins were first identified by their capacity to promote endochondral bone formation, they are involved in the cascades of body patterning and morphogenesis. Furthermore, BMPs play important roles after birth in the pathophysiology of several diseases, including osteoporosis, arthritis, pulmonary hypertension, and kidney diseases.[2]

Bone morphogenetic protein-7 is a 35-kDa homodimeric protein, and kidney is the major site of BMP-7 synthesis during embryogenesis as well as in postnatal development. *BMP-7*-deficient mice die shortly after birth due to severe renal hypoplasia.[3,4] Mutant kidneys suffer gradual cessation of nephrogenesis, associated with a reduction in ureteric bud branching and loss of metanephric mesenchyme, indicating that BMP-7 is essential for survival and differentiation of mesenchymal cells in kidney development.[5] In postnatal life, many developmental features are recapitulated during renal injury, and BMP-7 has been shown to be important in both preservation of kidney function and resistance to injury. For example, BMP-7 inhibits tubular epithelial cell dedifferentiation,[6–10] mesenchyme transformation, and apoptosis stimulated by various renal injuries, and has an anti-inflammatory effect in models of both acute and chronic renal failure.[11]

The local activity of endogenous BMP-7 is controlled not only by the precise regulation of its expression, but also by certain classes of molecules that bind to BMP-7, acting as positive[12] or negative regulators of BMP-7 activity in the kidney.[2,13–15] BMP antagonists function through direct association with BMP, thus inhibiting the binding of BMP to its receptors, and define the boundaries of BMP activity.

Recently, we found that the product of uterine sensitization-associated gene-1 (USAG-1) acts as a kidney-specific BMP antagonist, and that USAG-1 binds to and inhibits the biological activity of BMP-7.[16] We further demonstrated that *USAG-1*-deficient mice are resistant to kidney injury, and that USAG-1 is the central negative regulator of BMP

function in the adult kidney.[17] Because the interaction between BMP-7 and USAG-1 seems to play critical roles in the kidney, we analyzed the balance between USAG-1 and BMP-7 expression in kidney injury and development, and demonstrated the reciprocal relationship between USAG-1 and BMP-7 expression in kidney injury and development. Close examination of USAG-1 expression in developing kidneys further provided a clue to proximal–distal differentiation mechanism of nephron by demonstrating the possibility that each single cell in an immature nephron controls its own fate to become proximal or distal tubule cell. In addition, USAG-1 expression in the kidney biopsy could be a powerful diagnostic tool to predict renal prognosis.

RESULTS

Generation of *USAG-1*$^{+/LacZ}$ knock-in mice

To facilitate the temporal and spatial analyses of USAG-1 expression, we generated in-frame *USAG-1*$^{+/LacZ}$ mice. In our previous work, the nuclear *lacZ* reporter gene that was knocked in[17] proved unsuitable for signal detection. In this work, the cytoplasmic *lacZ* reporter gene was used to replace the open reading frame of *USAG-1* and create a novel knock-in allele (Figure 1a). While *USAG-1*$^{+/LacZ}$ mice showed no overt defects, *USAG-1*$^{LacZ/LacZ}$ mice presented the same teeth phenotype as observed in the original *USAG-1* mutants.[17] *In situ* hybridization (ISH) of a *USAG-1* antisense probe to whole embryos at E9.5 and adult kidney specimen confirmed that lacZ staining in *USAG-1*$^{+/LacZ}$ mice reflected authentic *USAG-1* gene expression (Figure 1d).

USAG-1 is expressed in distal tubules and overlaps with BMP-7 in distal convoluted tubules

To further analyze the localization of USAG-1 expression in the kidney, we used several well-characterized segment markers. First, we clarified the segments in which well-known segment markers are expressed (Figure 2a). Tamm Horsfall glycoprotein (THP) was expressed in thick ascending limb. The calbindin D28K was expressed in distal convoluted tubules (DCTs) and connecting tubules (CTs). Using the antibody from Upstate, NaKATPase α-1 subunit was strongly expressed in thick ascending limb, DCT, and CT. AQP-1 was expressed in proximal tubules, descending thin limb, and possibly in ascending thin limb, while AQP-2 was expressed in the collecting ducts (CDs)[18] and CTs as reported.

Next, we analyzed the localization of USAG-1 in adult kidneys using these markers, and demonstrated that all the tubules expressing calbindin D28K or THP in the cortex expressed USAG-1 (Figure 2b and c). In the outer medulla, USAG-1 expression completely overlapped with THP (Figure 2d) and NaKATPase (Figure 2e), but not with AQP-2 (Figure 2f) or AQP-1 (Figure 2g). In addition, USAG-1 expression in the cortex did not overlap with AQP-2 (Figure 2f) or AQP-1 (Figure 2g), except for CTs, which were double positive for *lacZ* transcript and AQP-2 (data not shown). In the inner medulla, USAG-1 expression was not detected (Figure 1d). From these findings, we concluded that USAG-1 is predominantly expressed in the distal tubules, more specifically, in thick ascending limb, DCT, and CT in adult kidneys.

For comparison, the expression of BMP-7 was determined using *BMP-7*$^{+/LacZ}$ mice, and the tubules expressing calbindin D28K (Figure 2h) or AQP-2 (data not shown) were positive for *lacZ* transcript, indicating that BMP-7 is expressed in DCT, CT, and CD as previously reported (Figure 2a).[11]

USAG-1 emerges in developing nephrons and colocalizes with BMP-7 only in differentiated tubules

Next, we examined the expression of USAG-1 and BMP-7 in kidney development. The expression of USAG-1 increased toward the later stage of development, and peaked at E17.5, while BMP-7 was constantly expressed during kidney development and decreased at perinatal period (Figure 3a). As a result, the ratio between USAG-1 and BMP-7 expression increased significantly toward the later stage of development (Figure 3a). We also compared the ratio between other BMP antagonists and BMP-7, and demonstrated that USAG-1 is predominantly the major BMP antagonist during kidney development (Figure 3a). At E13.5, USAG-1 expression was almost absent (Figure 3b), while BMP-7 expression was intensely expressed in ureteric buds, adjacent metanephric mesenchyme, and part of comma-shaped body (Figure 3c). At E15.5, USAG-1 expression was still absent in the comma-shaped body, but was strongly detected in more differentiated tubular epithelial cells in the medulla, in a pattern similar to that of BMP-7, except for the expression in the podocyte layers of the developing glomeruli, where USAG-1 expression was absent (Figure 3b and c). Therefore, we conclude that USAG-1 emerges in developing nephrons and colocalizes with BMP-7 only in differentiated tubules (Figure 3d). We also examined the expression of several segmental markers in *USAG-1*-deficient kidney to determine whether the developmental process is modified; however, we could not observe any difference in the expression pattern of these markers (data not shown).

Mosaicism of proximal tubule marker-positive cell and distal tubule marker-positive cell in a single immature nephron

From E17.5 to the neonatal period, two patterns of USAG-1 expression were observed in the kidneys: a strong signal in distal tubules (Figure 3b, arrowheads) and a weak, patchy signal in the cortex (Figure 3b, arrows). To demonstrate that both signals were not due to endogenous β-galactosidase activity in the kidney, kidneys of wild-type mice were subjected to lacZ staining and incubated for the same period of time, but no signal was detected (Figure 3b).

We further analyzed the property of these signals with segment markers, and found that the strong signal in neonatal *USAG-1*$^{+/LacZ}$ kidneys colocalized with THP and NaKATPase (Figure 4a and b), but not with AQP-1 or AQP-2 (Figure 4c and d). Calbindin D28K was hardly detected in the

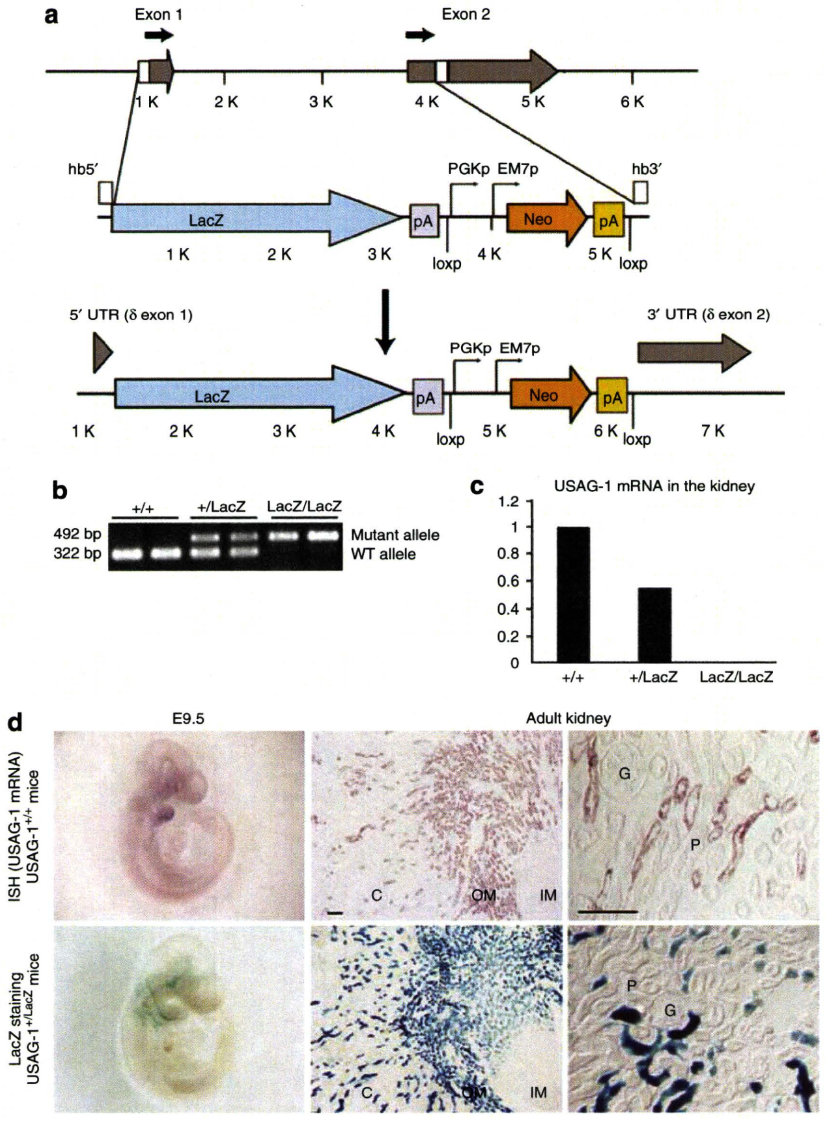

Figure 1 | Generation of USAG-1 $^{+/LacZ}$ knock-in mice by gene targeting. (**a**) Design of *Sostdc1* (gene symbol for *USAG-1*) null allele with concomitant replacement by LacZ. Light gray arrows depict the two exons; black arrows indicate the coding sequence. The homology boxes used for bacterial homologous recombination (BHR) are depicted as white (hb5′ and hb3′). The entire coding sequence of *Sostdc1* was replaced by LacZ/Neo, in a manner such that the initiating ATG of *Sostdc1* became the ATG of LacZ. The reporter open reading frame (ORF), LacZ, is followed by an SV40 polyadenylation signal and SV40-derived associated sequence[31] (purple boxes), whereas, the Neo ORF is followed by the mouse PGK polyadenylation signal and associated sequence[32] (yellow boxes). All of these elements are standard elements used by Velocigene.[29] The replacement afforded into the *Sostdc1* BAC by BHR is also translated in an identical manner into the mouse genome during targeting. Therefore, all the features shown above are also those present in the modified *Sostdc1* locus in the targeted embryonic stem (ES) cells. (**b**) PCR genotyping of *USAG-1* $^{+/+}$, *USAG-1* $^{+/LacZ}$, and *USAG-1* $^{LacZ/LacZ}$ littermates. (**c**) Real-time RT-PCR analysis of *USAG-1* mRNA in the kidneys of *USAG-1* $^{+/+}$, *USAG-1* $^{+/LacZ}$, and *USAG-1* $^{LacZ/LacZ}$ littermates. Expression of *USAG-1* was normalized to that of *GAPDH* and expressed relative to that in *USAG-1* $^{+/+}$ mice. (**d**) ISH of whole embryo and adult kidney section revealed a similar distribution of *USAG-1* mRNA and *lacZ* transcripts. C, cortex; OM, outer medulla; IM, inner medulla; P, proximal tubule; G, glomerulus. Bar = 100 μm.

immature nephron at this stage. On the other hand, only the weak, patchy signal, but not the strong signal, colocalized with the expression of the lectin-binding sites for Lotus Tetragonolobus Agglutnin (LTA) (Figure 4e), the marker for proximal tubules.[19] NDRG1, the cytoplasmic protein upregulated in several stress stimuli,[20] is known to be expressed in the proximal tubules and CDs in the kidney.[21] The weak, patchy signal of lacZ staining also colocalized with NDRG1 expression (Figure 4f), indicating that these tubules with weak, patchy signal of lacZ staining possess proximal tubule property, as well. AQP-1 was partially positive in the descending part of weak, patchy blue tubules (Figure 4d), possibly indicating that these tubules might have the characteristics of proximal tubules and thin limbs of Henle.

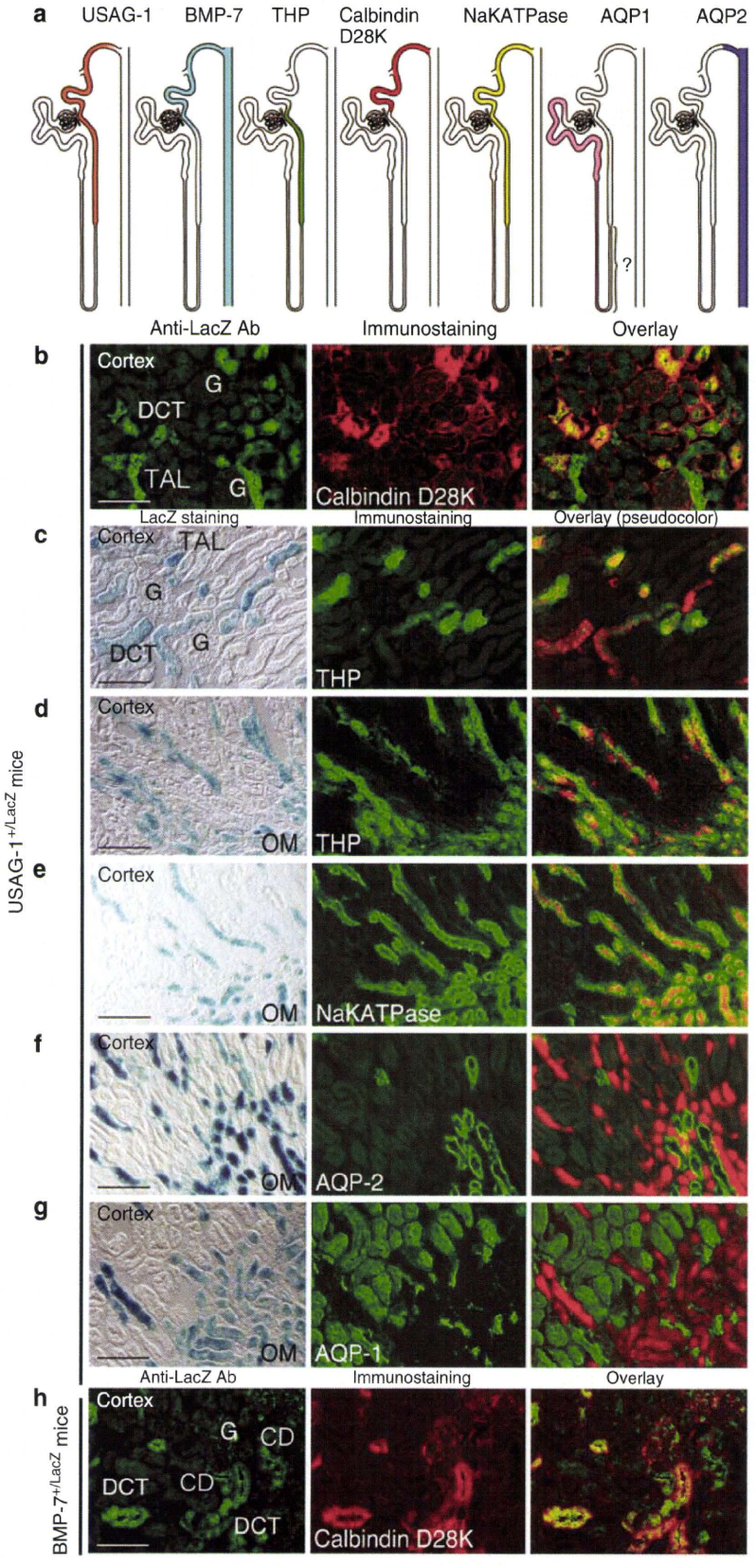
a
USAG-1
BMP-7
THP
Calbindin D28K
NaKATPase
AQP1
AQP2
?
Anti-LacZ Ab
Immunostaining
Overlay
b
Cortex
G
DCT
TAL
G
Calbindin D28K
LacZ staining
Immunostaining
Overlay (pseudocolor)
c
Cortex
TAL
G
DCT
G
THP
d
Cortex
OM
THP
e
Cortex
OM
NaKATPase
f
Cortex
OM
AQP-2
g
Cortex
OM
AQP-1
Anti-LacZ Ab
Immunostaining
Overlay
USAG-1+/LacZ mice
h
Cortex
G
CD
DCT
CD
DCT
Calbindin D28K
BMP-7+/LacZ mice

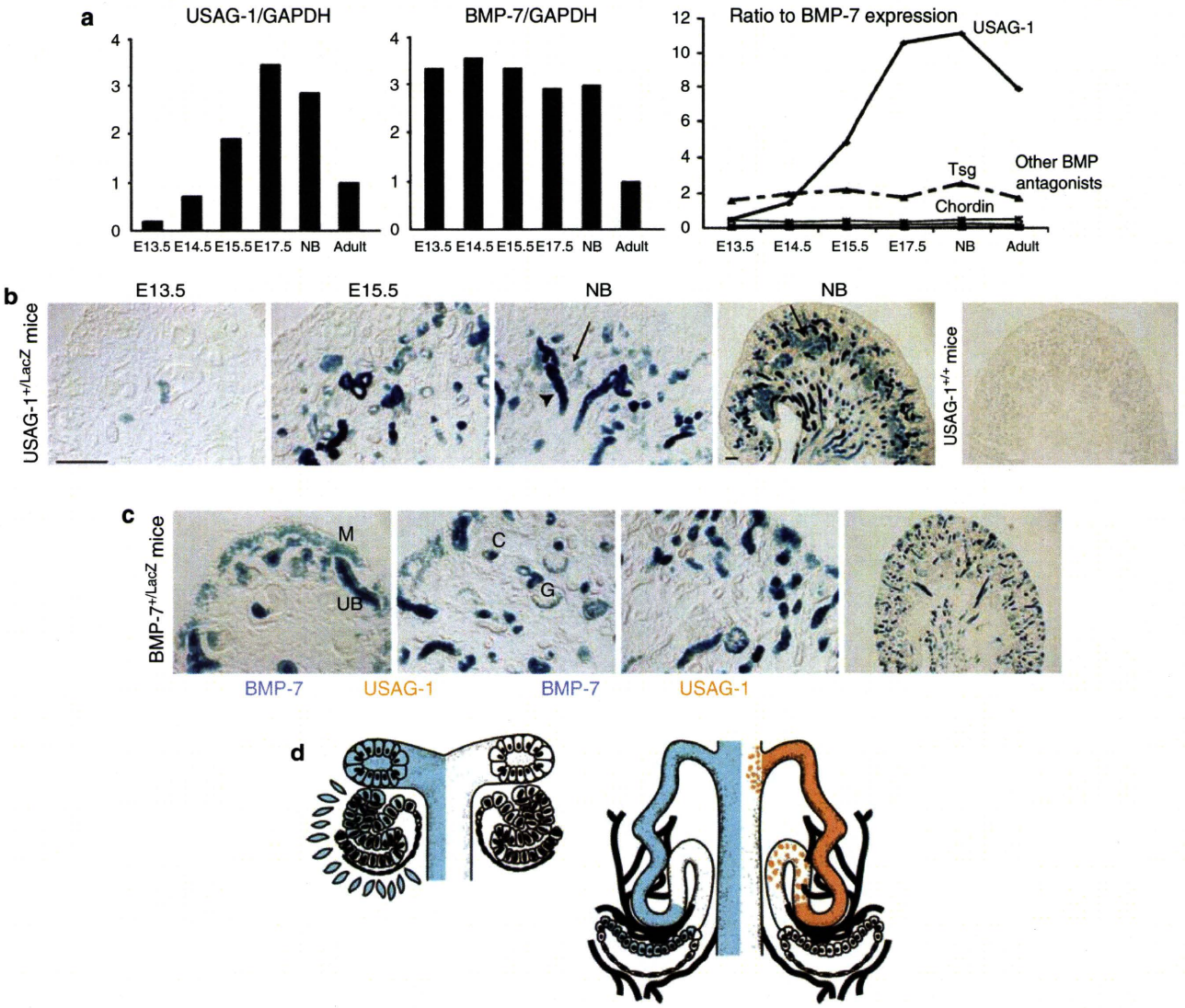

Figure 3 | USAG-1 emerged in developing nephrons and colocalized with BMP-7 in differentiated tubules. (**a**) Expression of USAG-1 and ratio of USAG-1/BMP-7 expression increased in kidney development. Metanephric kidneys from five to six embryos at indicated time points, and kidneys from seven neonates were collected and subjected to RNA extraction. Expression levels of USAG-1 and BMP-7 were normalized to the expression of GAPDH and expressed relative to the expression level in the adult kidney. The ratio of USAG-1 and other BMP antagonists to BMP-7 expression was determined as described (see Materials and Methods). (**b** and **c**) Localization of *lacZ* transcripts in developing *USAG-1*$^{+/LacZ}$ (**b**) and *BMP-7*$^{+/LacZ}$ (**c**) kidneys. Expression of *USAG-1/lacZ* transcripts did not emerge in immature nephrons, where BMP-7 facilitates differentiation, but was strong and overlapped with that of BMP-7 in the fully differentiated tubules (arrowheads). Besides, the strong signal of *USAG-1/lacZ* transcripts in distal tubules (arrowhead), a weak, patchy signal was observed in the neonatal kidneys (arrows). UB, ureteric bud; M, mesenchyme; C, comma-shaped body; G, glomerulus. Bar = 100 μm. (**d**) Schematic illustration demonstrating the expression of USAG-1 and BMP-7 during kidney development. USAG-1 expression was negative in the immature nephron, where BMP-7 was strongly expressed and promoted differentiation. USAG-1 expression emerged in more differentiated tubules and overlapped with that of BMP-7.

Figure 2 | USAG-1 and BMP-7 overlap in DCTs. (**a**) Schematic illustration demonstrating the expression of USAG-1, BMP-7, and other segment markers in the nephron. USAG-1 is expressed in thick ascending limb (TAL), DCTs, and in CTs, while BMP-7 is expressed in DCT, CT, and in CD. (**b**) Tubules positive for calbindin D28K are positive for *LacZ* transcripts in the kidneys of *USAG-1*$^{+/LacZ}$ mice. G, glomerulus. Bar = 100 μm. (**c**) Tubules positive for THP in the cortex are positive for *LacZ* transcripts in the kidneys of *USAG-1*$^{+/LacZ}$ mice. (**d**) Tubules positive for THP in the cortex and medulla are positive for *LacZ* transcripts in the kidneys of *USAG-1*$^{+/LacZ}$ mice. OM, outer medulla. (**e**) Tubules positive for NaKATPase in the cortex and medulla are positive for *LacZ* transcripts in the kidneys of *USAG-1*$^{+/LacZ}$ mice. (**f** and **g**) Tubules positive for AQP-2 (**f**) or AQP-1 (**g**) are negative for *LacZ* transcripts in the kidneys of *USAG-1*$^{+/LacZ}$ mice. (**h**) Tubules positive for calbindin D28K are positive for *LacZ* transcripts in the kidneys of *BMP-7*$^{+/LacZ}$ mice. *LacZ* transcripts in the kidneys of *BMP-7*$^{+/LacZ}$ mice are also positive in CD and podocyte in glomeruli.

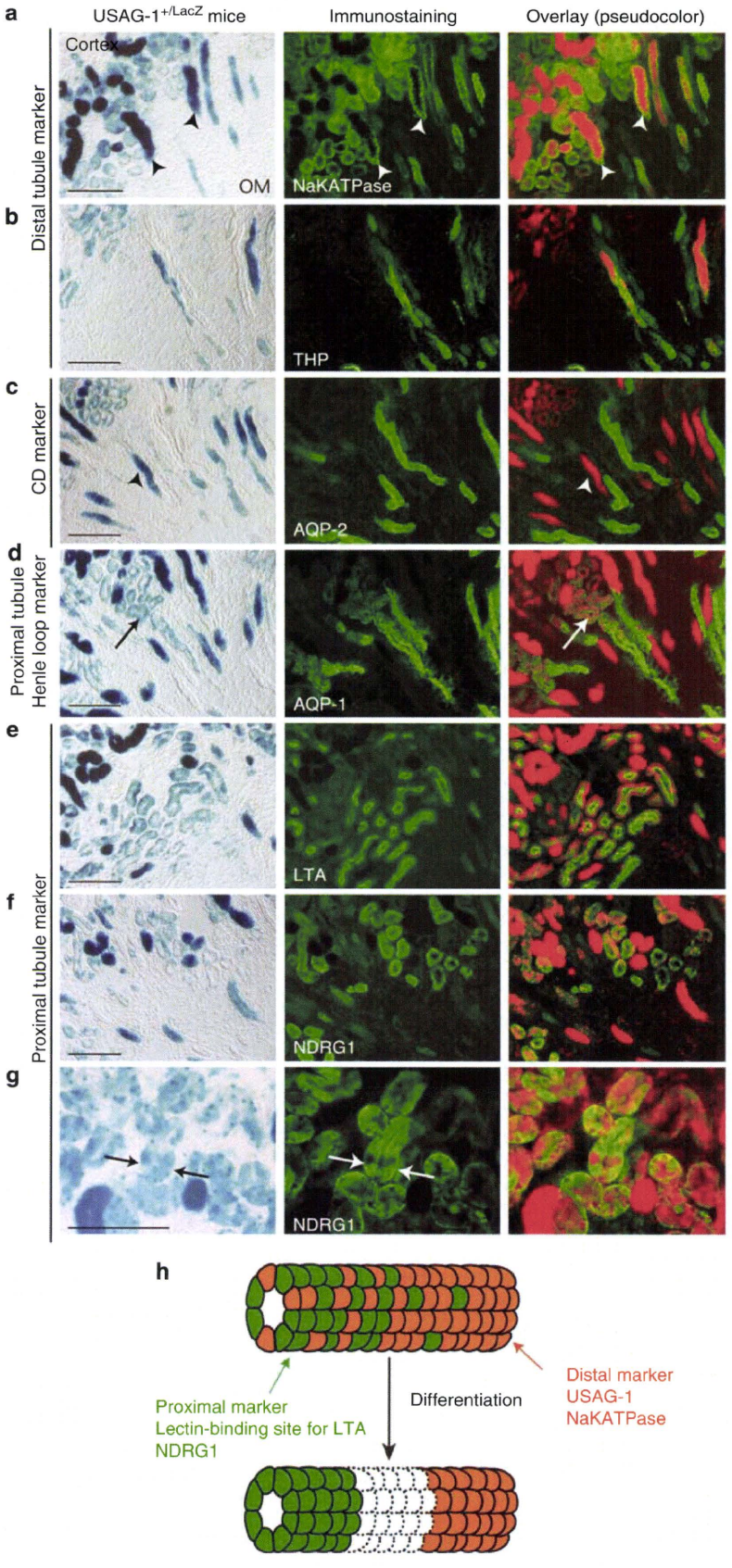
a
USAG-1+/LacZ mice
Immunostaining
Overlay (pseudocolor)
Cortex
OM
NaKATPase
Distal tubule marker
b
THP
c
CD marker
AQP-2
d
Proximal tubule
Henle loop marker
AQP-1
e
LTA
f
Proximal tubule marker
NDRG1
g
NDRG1
h
Proximal marker
Lectin-binding site for LTA
NDRG1
Differentiation
Distal marker
USAG-1
NaKATPase

Close examination of these tubules further clarified that the weak, patchy signal of lacZ staining and NDRG1 signals were not overlapping in a single cell, but were complementary in the single tubule (Figure 4g); therefore, the tubule in this area was made up of two types of epithelial cells: those with distal tubule property and those with proximal tubule property (Figure 4h). To exclude the possibility that lacZ staining quenches the fluorescence of other markers, immunostaining of the serial sections was performed and demonstrated similar results (data not shown).

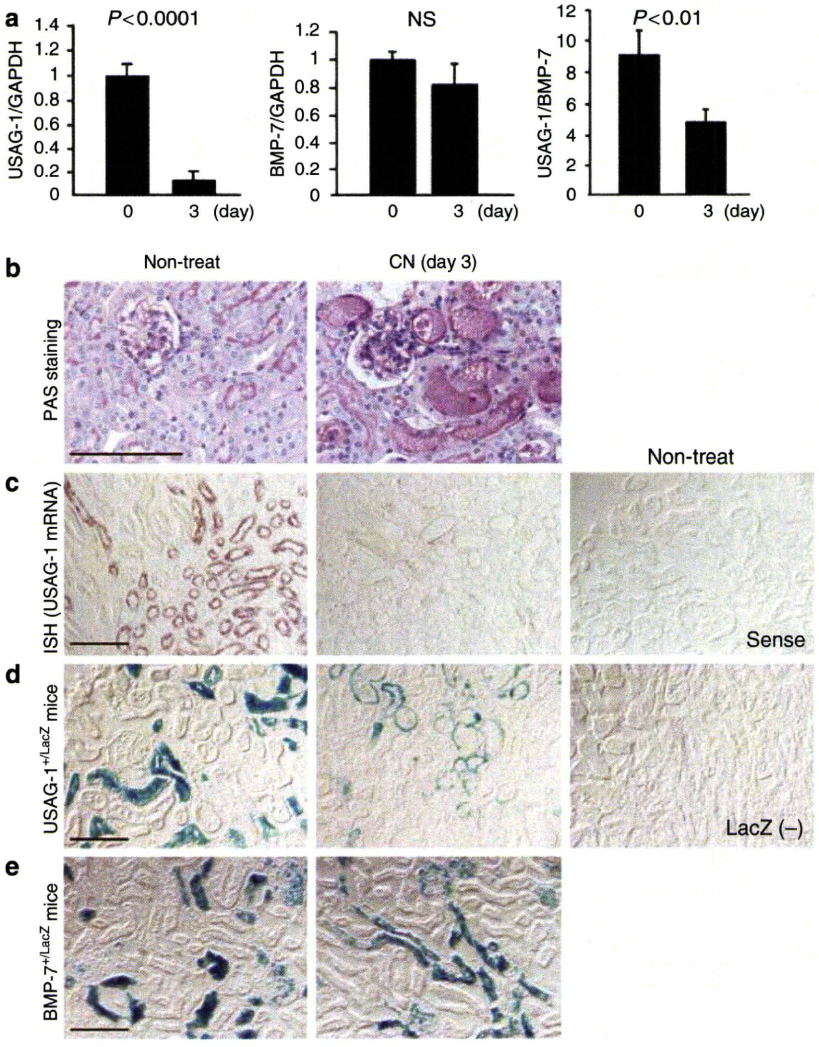

Figure 5 | Expression of USAG-1 decreased in tubular injury. (**a**) Expression of *USAG-1* mRNA decreased in acute tubular injury. Expression of USAG-1 and BMP-7 and the ratio between USAG-1 and BMP-7 expression during cisplatin nephrotoxicity (CN) were determined by real-time RT-PCR. Expression of USAG-1 and BMP-7 was normalized to that of GAPDH and expressed relative to that in mice on day 0. The ratio between USAG-1 and BMP-7 expression was determined by setting the standard curve with plasmids encoding each gene at various concentrations and analyzing the copy number of each gene contained in kidney cDNA (see Results). $N = 4$–6 for each experiment. (**b**–**e**) Representative histological findings (**b**), ISH of *USAG-1* mRNA (**c**), and lacZ staining of the *USAG-1*$^{+/LacZ}$ (**d**), and *BMP-7*$^{+/LacZ}$ (**e**) kidneys during CN. Bar = 100 μm.

Figure 4 | Mosaicism of proximal tubule marker-positive cell and distal tubule marker-positive cell in a single immature nephron. (**a**) Strong (arrowheads) and weak, patchy signal of *lacZ* transcripts in neonatal *USAG-1*$^{+/LacZ}$ kidneys colocalized with NaKATPase. Bar = 100 μm. (**b**) Strong signal of *lacZ* transcripts in neonatal *USAG-1*$^{+/LacZ}$ kidneys colocalized with THP. (**c**) *LacZ* transcripts in neonatal *USAG-1*$^{+/LacZ}$ kidneys did not colocalize with AQP-2. (**d**) AQP-1 was partially positive in the descending tubules with weak, patchy signal of *lacZ* transcripts (arrow). (**e**) Weak, patchy signal of *lacZ* transcripts colocalized with lectin-binding sites for Lotus Tetragonolobus Agglutnin (LTA). (**f**) Weak, patchy signal of *lacZ* transcripts colocalized with NDRG1. (**g**) Close examination of the overlapping areas demonstrated that the weak, patchy signal of *lacZ* transcripts (arrows) was not overlapping with NDRG1 expression, but was complementary in a single tubule. (**h**) Working hypothesis for proximal-distal differentiation mechanism of kidney tubules. Proximal tubule marker-positive cells (green) lie side by side with distal tubule marker-positive cells (red) in a single immature nephron. It is postulated that each single cell possesses its cell fate to become proximal or distal tubular cell.

The ratio between USAG-1 and BMP-7 expression was reduced in tubular injury and increased in tubular regeneration

We also examined the expression of USAG-1 and BMP-7 in kidney injury. Administration of cisplatin causes acute tubular necrosis and apoptosis, leading to deterioration of renal function. USAG-1 but not BMP-7 mRNA in the kidney decreased at day 3 of cisplatin nephrotoxicity (Figure 5a). ISH and lacZ staining demonstrated that USAG-1 expression was significantly reduced at day 3 of cisplatin nephrotoxicity, while the lacZ staining in *BMP-7*$^{+/LacZ}$ mice was maintained (Figure 5c–e). At day 0 of cisplatin nephrotoxicity, the expression level of USAG-1 was much higher than that of BMP-7, but at day 3, the ratio between USAG-1 and BMP-7 expression was significantly decreased, indicating that the reduction of USAG-1 expression was more prominent than that of BMP-7.

Next, we examined the expression of USAG-1 in the kidney regeneration. Administration of folic acid (FA) to mice causes intratubular crystallization, which results in dilatation and degeneration of tubules, leading to transient acute renal failure[22] (Figure 6a). In contrast to the cisplatin nephrotoxicity model, damaged tubular epithelial cells proliferate and regenerate after several days, and renal function returns to normal by day 14 (Figure 6a). Expression of USAG-1 in this model decreased during tubular epithelial damage (day 1), but increased markedly during proliferation and regeneration of tubular epithelial cells (days 7–10), and

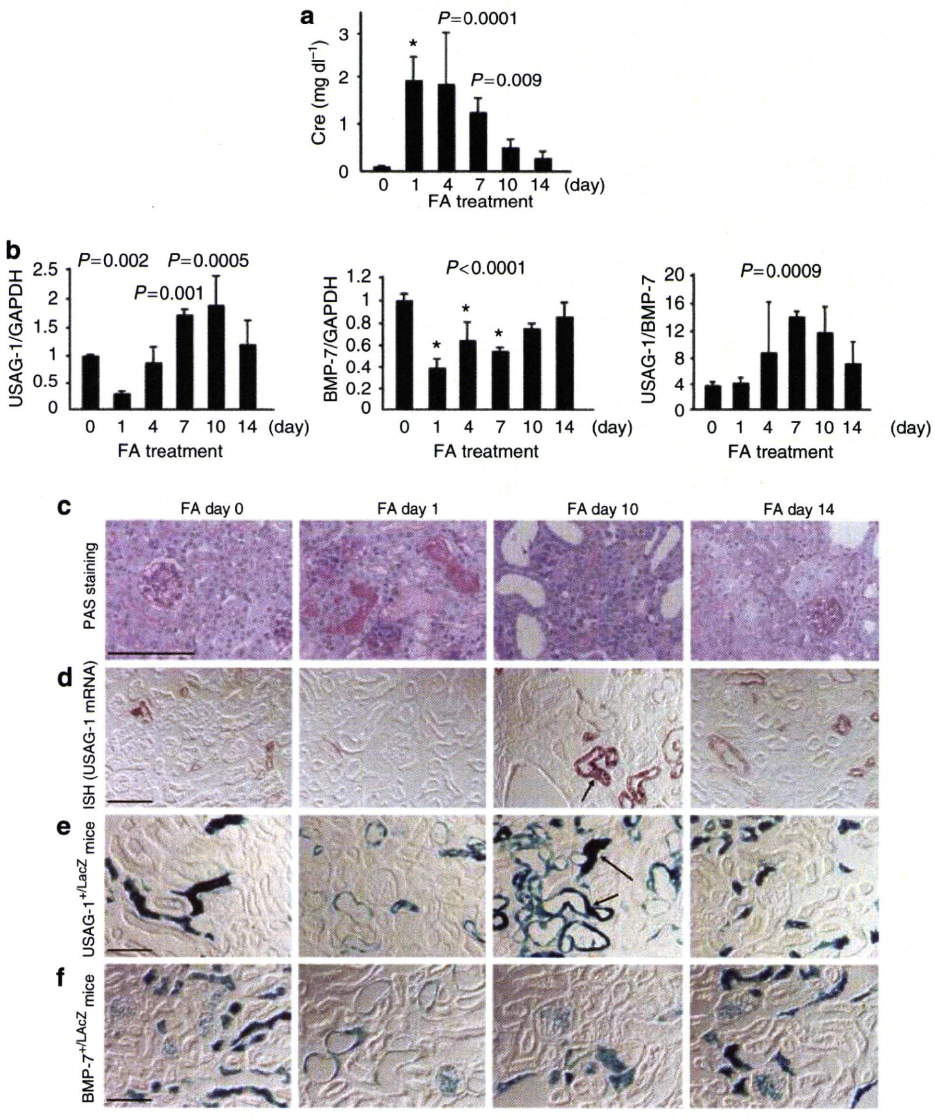

Figure 6 | Expression of USAG-1 increased in tubular regeneration. (**a**) Time course of serum creatinine level in FA nephrotoxicity model. (**b**) Expression of USAG-1 and BMP-7 and the ratio between USAG-1 and BMP-7 expression after FA treatment. $N = 4$–6 for each experiment. (**c**–**f**) Representative histological findings (**c**), ISH of USAG-1 mRNA (**d**), and lacZ staining of the *USAG-1*$^{+/LacZ}$ (**e**) and *BMP-7*$^{+/LacZ}$ kidneys (**f**) after FA treatment. Bar = 100 μm. USAG-1 was strongly detected in the irregularly lined regenerating epithelial cells (**d** and **e**; arrows).

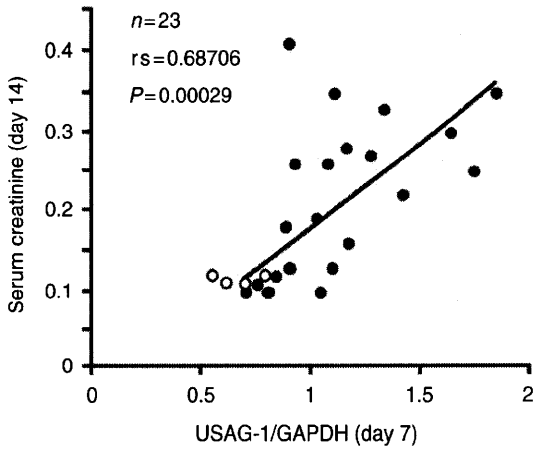

Figure 7 | USAG-1 as a diagnostic marker for renal prognosis. A significant correlation is observed between *USAG-1* expression in kidney biopsy sample at day 7 and serum creatinine at day 14 in FA nephrotoxicity (closed circle, $N=23$). Open circles indicate control kidneys without FA nephrotoxicity ($N=4$).

returned to the basal level when redifferentiation of tubular epithelial cells was completed (day 14), while the expression of BMP-7 increased gradually after the initial dip at day 1 (Figure 6b). ISH and lacZ staining demonstrated that USAG-1 was strongly detected in the irregularly lined regenerating tubular epithelial cells at day 10 (Figure 6d and e, arrows), which might account for the increase in USAG-1 expression at this time point (Figure 6b). The ratio between USAG-1 and BMP-7 expression was significantly increased during the regeneration phase (Figure 6b). We also compared the ratio between other BMP antagonists and BMP-7 in both kidney disease models, and demonstrated that USAG-1 is predominantly the major BMP antagonist during kidney injury (Figure S1).

USAG-1 as a predictive marker for renal prognosis

Because USAG-1 is a negative regulator of the renoprotective action of BMP-7, we postulated that high expression of USAG-1 in the kidney biopsy might predict poor renal prognosis.

Because regenerating tubules and damaged tubules are observed in the regenerating period (days 7–10) of FA nephrotoxicity and might mimic the situation in the clinical kidney biopsy specimen, we utilized the model and performed kidney biopsy at day 7 and examined renal function at day 14. Interestingly, the expression of USAG-1 in kidney biopsy at day 7 correlated significantly with renal function at day 14 (Figure 7), indicating the possibility that USAG-1 could be a predictive marker of renal prognosis. We also performed renal biopsies at days 1 and 10. As shown in Figure S2, USAG-1 expression at day 10 ($N=4$, regenerating period) correlated well with future renal function at day 14, while USAG-1 expression at day 1 ($N=8$, tubular damage period) did not. Therefore, we conclude that USAG-1 expression correlated well with future renal function when tubular regeneration is observed.

DISCUSSION

USAG-1 colocalizes with BMP-7 only in differentiated tubules in developing kidney

During kidney development, BMP-7, made by both metanephric mesenchyme and tubular epithelial cells (Figure 3c), is a facilitator of ureteric bud branching at low concentrations, but an inhibitor of branching at high concentrations.[23] The discrepancy is a part of a feedback mechanism that allows ureteric buds to branch into 'unpopulated' areas of mesenchyme, but not into areas already populated by nephrons and other bud branches. USAG-1 expression did not emerge in immature nephrons where BMP-7 facilitates differentiation, but was strongly expressed and overlapped with BMP-7 in fully differentiated tubules (Figure 3b and c). We also demonstrated that USAG-1 expression is lower than that of BMP-7 at E13.5, is comparable at E14.5 and E15.5, and is much higher at E17.5 and in newborns (Figure 3a). In addition, USAG-1 is the major BMP antagonist during kidney development (Figure 3a). These data support the idea that USAG-1 might function as a feedback mechanism for BMP-7 activity during kidney development. However, no developmental abnormality was observed in the kidney of *USAG-1*-deficient mice,[17] and some redundant factor might overcome the lack of USAG-1 in the kidney of *USAG-1*-deficient mice during development. Twisted gastrulation is one candidate for the redundancy, because the expression pattern is similar to that of USAG-1 and the expression level is the second highest among BMP antagonists to USAG-1 (Figure 3a).

USAG-1 expression gives an insight into proximal–distal differentiation mechanism of immature nephron

In spite of that USAG-1 expression was confined to distal tubules in adult kidney, weak, patchy expression of USAG-1 in neonatal kidneys colocalized with proximal tubular markers, such as lectin-binding site for Lotus Tetragonolobus and NDRG1 in the cortex. NaKATPase, another distal tubule marker, also colocalized with proximal tubular markers in the area (data not shown). AQP-1 was partially positive in the descending part of weak, patchy blue tubules, possibly indicating that these tubules might also have the property of proximal tubules and thin limbs of Henle. Close examination of the area double positive for proximal and distal markers further demonstrated that each single cell is not double positive for these two markers, but two types of cells positive for each marker intermingled with each other in a single tubule (Figure 4g and h). Little is known about the mechanism how uniform mesenchymal cells differentiate to a variety of cells, including glomerular epithelial cells, proximal tubular cells, and distal tubular cells, along the proximal–distal axis.[24] There has been a controversy between the following two hypotheses: gradient of growth factors brings the proximal–distal differentiation, or cell fate is determined for each cell. Recent studies revealed critical roles of Notch in the determination of proximal tubule cells and the fates of podocytes.[25–27] Our data might support the cell fate